

NASA CR-134878

DESIGN AND FABRICATION OF
SILVER-HYDROGEN CELLS

by M. G. Klein

ENERGY RESEARCH CORPORATION

prepared for

NATIONAL AERONAUTICS AND SPACE ADMINISTRATION

NASA Lewis Research Center
Contract NAS 3-18543

TABLE OF CONTENTS

	<u>Page</u>
1. SUMMARY	1
2. INTRODUCTION	1
3. RESULTS AND DISCUSSION	2
4. FINAL DESIGN	33
4.1 Cell Description	33
4.2 Electrode Stack	36
4.3 Cell Hardware	38
4.4 Cell Design	40
5. DESIGN, FABRICATION AND TEST OF 20Ahr CELLS	46
6. CONCLUSIONS	60

DESIGN AND FABRICATION OF SILVER-HYDROGEN CELLS

M. G. Klein

1. SUMMARY

This report presents the results obtained under a Research and Development contract for the development and fabrication of silver-hydrogen secondary cells. The program consisted of an experimental task utilizing single electrode pairs for the optimization of the individual electrode components, the preparation of a design for lightweight 20Ahr cells and the fabrication of four 20Ahr cells in heavy wall test housings containing electrode stacks of the lightweight design for delivery to NASA Lewis.

The active elements consist of a PFE fuel cell anode and NASA Astropower Separator Material which were GFE, an inter-cell electrolyte reservoir and sintered silver electrodes. The 20Ahr cell design utilized the cylindrical cell concept in which a stack of disc electrodes is contained. The free volume within the cylinder accommodates the hydrogen gas which is generated on charge. The individual electrode pair tests demonstrated the initial performance capabilities of the system and led to the selection of a .076cm (30 mil) thick silver electrode for the final cell design. Four 20Ahr cells in heavy wall housings were assembled and subjected to five acceptance cycles and demonstrated rated performance.

2. INTRODUCTION

This report is submitted to NASA/Lewis under Contract NAS3-18543 for the design and fabrication of silver-hydrogen secondary cells that are capable of delivering higher energy densities than comparable nickel-cadmium and nickel-hydrogen cells and relatively high cycle life. The cells should also be capable of being insensitive to overcharge and overdischarge. The design approach is based on the use of a single cylindrical self-contained cell with a stacked disc sequence of electrodes. The electrode stack design is based on the use of NASA - Astropower Separator Material, PPF fuel cell anodes, an intercell electrolyte reservoir concept and sintered silver electrodes. The overall 9 month program was broken down into the following tasks.

TASK I - Design

The preparation of an initial paper design of a single 20Ahr silver-hydrogen cell.

TASK II - Design Testing

The experimental investigation of single electrode test cells for the demonstration of feasibility of performance and the optimization of the individual electrode components.

TASK III - Final Design

The updated of the 20 ampere-hour cell design based on the experimental results obtained in Task II.

TASK IV - Fabrication and Assembly

The fabrication and assembly of four 20 ampere-hour cells in conformance with the final design of Task III.

TASK V - Acceptance Testing

The conducting of electrical acceptance testing on the four cells which were then delivered to NASA/Lewis.

TASK VI - Reliability and Quality Assurance

The maintenance and calibration of test and data acquisition equipment, materials control, and preparation of materials and process specifications.

3. RESULTS AND DISCUSSION

Design Testing

In order to assist in the selection of a silver-hydrogen multi-electrode cell design, a series of experiments were conducted in heavy wall housings which contained one silver electrode and two hydrogen electrodes. Figure 1 shows a photograph of the test housing used. It consists of a lid and a base which has a cavity where the electrodes and hydrogen gas is contained. The lid contains two insulated feedthroughs, a pressure gauge, a valve and O-ring seal for easy disassembly.

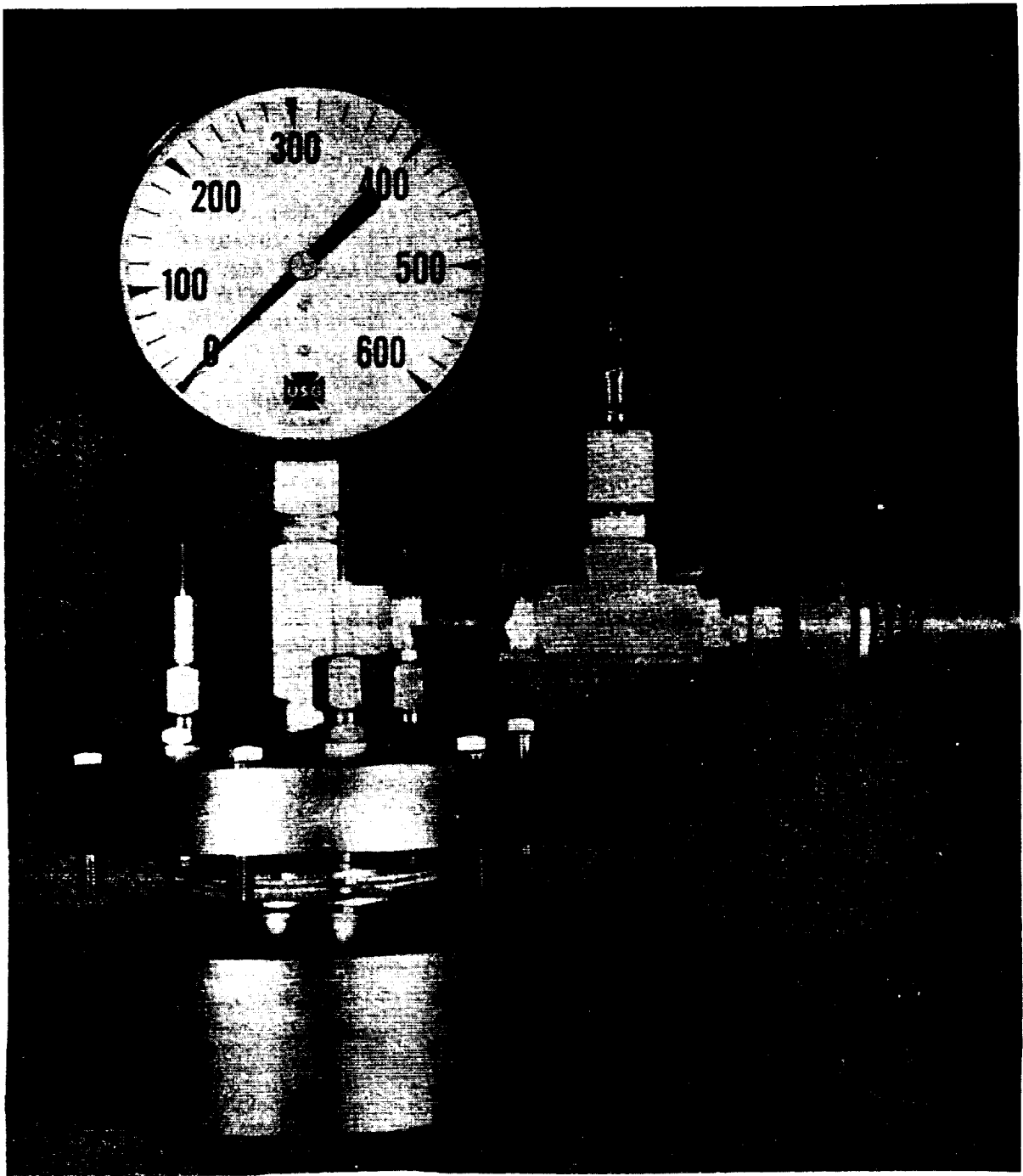


FIGURE 1 SINGLE ELECTRODE TEST CELL

The object of these test cells was to demonstrate feasibility of the electrodes matrix reservoir sandwich, filling procedures and to optimize the individual components. The initial group of cells was classified as "shake-down tests." Table 1 shows the construction variables of the cells fabricated during the program.

Cell 001 consisted of two hydrogen electrodes of the PPF type which are fuel cell type electrodes manufactured by Pratt & Whitney and supplied to ERC by NASA/Lewis. Separator 015 and 106.

One lot of fuel cell electrodes was used for the entire program (PCJ-560). The electrodes are Teflon bonded platinum black layer (9 mg/cm^2) on a silver plated nickel screen of approximately $100'' \times 100''$ mesh. The electrodes were stamped into the standard test size a 6.10 cm ($2.4''$) diameter with two flat chords 4.5 cm ($1\text{-}3/4''$) for current take offs.

The separator material consisted of one layer of NASA - Astropower separator $.4 \text{ mm}$ thick ($.016\text{--}.016''$) supplied by NASA/Lewis to ERC. One lot of separator was used for the entire program (#3D1574B). The separator was punched with an extended edge over the cell electrodes of $.158 \text{ cm}$ ($1/16''$). The silver electrode was of sintered powdered type containing a silver expanded metal fabricated at ERC. The initial silver electrodes contained a spot-welded silver wire as the current take off. The electrolyte reservoir was fabricated from porous sintered nickel plaque nominally $.066 \text{ cm}$ ($.026''$) thick 78% porous. The initial reservoir plaques contained integral nickel screen $20 \times 20 \times .018 \text{ cm}$ ($.007''$) which was available at the start of the program. A flow field was coined into one side of the electrolyte reservoir by pressing a piece of $20 \times 20 \times .018 \text{ cm}$ ($.007''$) screen into the nickel sinter at a pressure of $4,546 \text{ Kg}$ ($10,000 \text{ lb.}$). The electrolyte reservoirs weighed typically 3.5 grams and has an electrolyte take up of approximately 1.1 grams .

The cell stacking sequence consisted of a plastic endplate, the electrolyte reservoir, the fuel cell hydrogen electrode, the Astropower separator material with the ceramic side facing the fuel cell electrode and the silver electrode and then a repeating sequence on the other side of the silver electrode.

The cell was assembled between two plastic endplates and vacuum filled with 30% KOH and then subjected to a soak period overnight at 80°C . The cell was then charged in free electrolyte for 20 hours at $.2 \text{ amperes}$. The cell was then removed from the free electrolyte, towel dried, assembled in the boilerplate assembly, pressurized to 300 psi hydrogen and put on a $.5 \text{ ampere}$ discharge.

TABLE I
CELL CONSTRUCTION

Cell #	H ₂ Electrode	Separator	Silver Electrode Thickness (mm)	Theo. A. H.	Edge Seal	IER Thickness (mm)	Electrolyte Concentration %	wt. gains Initial (gms)	Electrolyte gms After Test
001	PPF	Astropower	.89	4.35	Extended Edge	.63	30	6.4	
001A	PPF (New)	Added Asbestos	.89	4.35	Extended Edge	.63			
002	PPF	Asbestos	.90	4.0	Extended Edge	.63	30	6.7	
003	PPF	Astropower	.90	4.3	Extended Edge	.64	25	5.70	5.15
004	PPF	Astropower	.96	4.65	Extended Edge	.64	25	6.05	5.20
005	PPF	Astropower	.91	4.8	Shrink Tubing	.64	25	6.74	6.37
006	PPF	Astropower	.96	4.8	Shrink Tubing	.68	25	6.50	5.97
007	PPF	Astropower	.84	4.9	Frame	.65	25		6.17
008	PPF	Astropower	.84	4.5	Frame	.63	25		6.38
009	PPF	Astropower	.85	4.7	Extended Edge	.61	25	6.33	
010	PPF	Astropower	.85	4.6	Extended Edge	.53	25	6.57	

TABLE I
(cont'd)

Cell #	H	Electrode	Separator	Silver Electrode Thickness (mm)	Theo. A. H.	Edge Seal	IER Thickness	Electrolyte Concentration %	Electrolyte wt. gains Initial (gms)	Electrolyte gms. After
011		PPF	Astropower	1.85	9.0	Extended Edge	1	25	10.1	9.38
012		PPF	Astropower	1.78	9.0	Extended Edge	1	25	10.0	9.1
013		PPF	Astropower	1.27	7.0	Extended Edge	.91	25	8.2	
014		PPF	Astropower	1.25	6.8	Extended Edge	.91	25	8.1	
015		PPF	Astropower	.63	3.5	Extended Edge	.63	25	5.48	
016		PPF	Astropower	.63	3.2	Extended Edge	.63	25	6.6	
017		PPF	Astropower	.78	3.5	Extended Edge	.55	25	Poor Initial Performance Due To Improper Filling	
018		PPF	Astropower	.76	3.5	Extended Edge	.55	25	"	"
019		PPF	Astropower	.78	3.5	Extended Edge	None	25	3.76	
020		PPF	Astropower	.80	3.6	Extended Edge	None	25	3.58	
021		PPF	Astropower	.78	7.0	Extended Edge	None	25	7.85	

TABLE I
(cont'd)

Cell #	H ₂ Electrode	Separator	Silver Electrode Thickness (mm)	Theo. A. H.	Edge Seal	IER Thickness (mm)	Electrolyte Concentration %	wt. gains Initial (gms)	Electrolyte gms. After
022	PPF	Astropower	.76	3.7	Extended Edge	.55	25	5.50	
023	PPF	Astropower	.78	3.7	Extended Edge	.58	25	6.54	
024	PPF	Astropower	.81	3.5	Extended Edge	None	20	3.5	
025	PPF	Astropower	.81	3.7	Extended Edge	None	20	3.4	
026	PPF	Astropower	.76	3.5	Extended Edge	.56	30	6.2	
027	PPF	Astropower	.76	3.6	Extended Edge	.56	30	6.4	
028	PPF	Astropower	.78	3.4	Extended Edge	.56	40	6.77	
029	PPF	Astropower	.80	3.6	Extended Edge	.56	40	6.9	
030	PPF	Astropower	.78	3.4	Extended Edge	.56	20	7.76	
031	PPF	Astropower	.78	3.4	Extended Edge	.56	20	7.12	

Table II shows a summary of the test results. On the first discharge the cell only delivered 1.08 ampere-hours. The cell was disassembled and inspected. The hydrogen electrode and the electrolyte reservoir were found to be very wet with the electrolyte. The cell was reassembled by adding another separator layer of asbestos which had been presoaked in electrolyte against the fuel cell electrode face and new hydrogen electrodes. The results were slightly improved but still poor.

Cell #002 was similar in construction to cell 001. The test results are shown in Table III and were similar to cell 002. After the first discharge, the separator was replaced with asbestos. After the second cycle the cell was found to be shorted.

Apparently, by charging the cells in free electrolyte the reservoir is full of electrolyte at the start of the first charges. As water is formed on the hydrogen electrode during the discharge, it does not transfer through the separator rapidly enough and results in hydrogen electrode flooding.

Cells #003 and 004 were similar in construction to cells 001 and 002 and were initially vacuumed filled with 25% potassium hydroxide electrolyte and soaked for 16 hours at 80°C. However, they were then removed from the free electrolyte, towel dried, assembled into the test cells, and put on the initial charge. The results of these cells are shown in Tables IV and V. The performance of both of these cells was acceptable and they exhibit flat operating voltages to the end of their capacity. The cells give relatively stable output over the discharge current range from .5 amps to 2 amps at a silver utilization of approximately 2.7 grams per ampere-hour.

To complete the shakedown testing, both cells were placed on an automatic cycle for 5 cycles which consisted of 10.8 hour charge at 250 milliamps and a 1.2 hour discharge at 2 amps. The results of the cells are as shown in Tables IV and V. After testing the cells were disassembled and examined. A final wet weight of the cells was taken and a weight loss was observed as shown in Table I. This is not considered critical since it is expected during initial testing some electrolyte will be ejected from the cell. Meaningful electrolyte loss could only be determined over extensive cycle testing which was beyond the scope of this program. Based on acceptable performance of Cells 003 and 004 the shakedown tests were considered complete and the next group of cells were directed at evaluating various separator edge seals.

Cells 005 and 006 contained a heat shrink edge band on top of the separators. Cells 007 and 008 had a frame of .15cm (.060") width that was epoxy cemented between the two separator layers around the silver electrode and Cells 009 and 010 contained a .13cm (.050") separator extended edge without any edge seal.

TABLE II

TEST RESULTS OF CELL #001

Cycle	Current (Amps)	Capacity (Ah)	Pressure (Start) (psi)	Pressure (Finish) (psi)	End Voltage (Volts)	Comments
C1	.2	4	---	---	1.71	
D1	.5	1.08	300	210	.75	
C2	.2	3.2	150	325	1.80	Added Asbest layer and Ne H ₂ Electrode
D2	.5	2.4	325	165	.75	
C3	.25		165	365	1.83	
D3	.5	3.33	365	90	.75	
C4	.25	4.0	90	355	1.83	
D4	.5	3.33	355	85	.75	

TABLE III

TEST RESULTS OF CELL #002

Cycle	Current (Amps)	Capacity (Ah)	Pressure (Start) (psi)	Pressure (Finish) (psi)	End Voltage (volts)	Comments
C1	.2	4	---	---	1.71	
D1	.5	.625	300	245	.75	
D1 cont.	.5	.79	300	260	.75	Replaced Sep. with Asbestos
C2	.2	3.2	150	200	1.84	
D2	.5	.33	200	125	.70	

TABLE IV
TEST RESULTS OF CELL #003

Cycle	Current (amps)	Capacity (Ah)	Pressure (Start) (psi)	Pressure (Finish) (psi)	End Voltage (volts)	Comments
C1	.1	4.9	50	280	1.69	
D1	.5	2.7	280	50	.75	
C2	.2	3.2	50	300	1.74	
D2	2	2.56	300	100	.75	
C3	.5	3.2	50	270	1.77	
D3	1.75	2.77	270	50	.75	
C4	.2	3.2	50	285	1.80	Fixed Hydrogen Leak in Test Cell
D4	1.25	3.4		60	.75	
C5	.2	3.2	60	3.0	1.75	
D5	.5	3.2	310	50	.75	
C6	.25	2.7			1.8	
D6	2	2.4			.95	
C7	.25	2.7			1.8	
D7	2	2.4			.95	
C8	.25	2.7			1.8	
D8	2	2.4			.95	
C9	.25	2.7			1.8	
D9	2	2.4			.95	
C10	.25	2.7			1.8	
D10	2	2.9			.75	

TABLE V
TEST RESULTS OF CELL #004

Cycle	Current (Amps)	Capacity (Ah)	Pressure (Start) (psi)	Pressure (Finish) (psi)	End Voltage (volts)	Comments
C1	.1	4.9	50	350	1.77	
D1	.5	3.12	350	50	.75	
C2	.2	3.2	50	350	1.70	
D2	2	2.9	350	50	.75	
C3	.2	3.2	50	350	1.74	
D3	1.75	3.4	350	60	.75	
C4	.2	3.2	50	330	1.72	
D4	1.25	3.3	330	50	.75	
C5	.2	3.2	50	320	1.71	
D5	.5	3.12	320	40	.75	
C6	.25	2.7			1.7	
D6	2	2.4			1.9	
C7	.25	2.7			1.8	
D7	2	2.4			1.0	
C8	.25	2.7			1.8	
D8	2	2.4			1.0	
C9	.25	2.7			1.8	
D9	2	2.4			.95	
C10	.25	2.7			1.8	
D10	2	3.0			.75	

The results of these cells are shown in Tables VI through XI. From the test results, it did not appear that any significant differences in performance resulted from the various edge seals. Cell 010 did develop a short on the third cycle which resulted in the discontinuation of its test. An examination of that cell revealed that in the assembly, the separator layer was off center, allowing for a contact between the positive and negative electrodes. This is not considered to be a poor reflection on the extended edge seal concept. With proper care that type of edge can be managed. Cells 005 and 006 with the edge band did have an unreacted dark silver oxide zone under the edge band, but the capacity outputs didn't show significant differences. No indications of any internal reactions were observed in any of the cells. Based on results obtained from other metal-gas program, it appears desirable to keep the positive electrode open such that no oxygen accumulations are possible. Therefore, the extended edge separator seal is favored and was selected for use in further rest cells. Questions concerning the possibility of silver bridging with the extended edge approach still remain. In the testing done thus far, no silver bridging was observed. At this point it could only be verified by extended cycle testing.

Figure 2 shows a family of discharge curves at the different rates tested for Cell 009. The operating voltages and capacity output can be considered fairly typical and representative of all the cells with similar construction, Cells 003 through 010. Cells 009 and 010 contained inter-cell electrolyte reservoirs that were fabricated specifically for the program and were sintered nickel powder which contained no screen. There didn't appear to be any difficulty in utilizing these electrolyte reservoirs and they performed satisfactorily.

The next series of test cells was directed at evaluating different silver electrode thicknesses. The characteristics of the individual silver-electrode as a function of thickness is a key factor in dictating the number of electrodes required for the 20Ahr cell design.

Cells 011 and 012 contain silver electrodes that were approximately twice as thick as the electrodes previously tested. The cells also incorporate thicker electrolyte reservoirs to store more electrolyte. Test results of these cells as shown in Table XII and XIII. It was initially intended to run these cells at twice the current as the previous test cells to keep the discharge periods the same. However, on the second discharge when the discharge current was to have been 4 amps, both cells exhibited an operating voltage below .75 volts at the start of the discharge. Therefore, the discharge current was reduced to the 2 amp level and the remaining tests were conducted at lower operating currents. The cells gave good capacity utilization of the silver at lower rates of discharge, but poor output at the higher current rates to the .75 volt endpoint. These results showed that 1.8mm (.070") thick

TABLE VI
Test Results of Cell #005

Cycle	Current (Amps)	Capacity (Ah)	Pressure (Start) (psi)	Pressure (Finish) (psi)	End Voltage (volts)	Comments
C1	.1	4.6	50	410	1.68	
D1	.500	3.73	410	60	.75	
C2	.200	3.11	80	360	1.66	
D2	1.25	2.93	360	80	.75	
C4	.2	3.09	80	360	1.66	
D4	.5	3.1	360	60	.75	
C5	.2	3.2	60	350	1.47	Open Circuit For 72 Hours
D5	.5	2.72	310	60	.75	
C6	.25	2.7			1.70	
D6	2	2.4			1.05	
C7	.25	2.7			1.80	
D7	2	2.4			1.05	
C8	.25	2.7			1.80	
D8	2	2.4			1.05	
C9	.25	2.7			1.80	
D9	2	2.4			1.05	
C10	.25	2.7			1.80	
D10	2	2.9			.75	

TABLE VII
Test Results of Cell #006

Cycle	Current (Amps)	Capacity (Ah)	Pressure (Start) (psi)	Pressure (Finish) (psi)	End Voltage (volts)	Comments
C1	.1	4.6	50	390	1.68	
D1	.5	3.72	390	60	.75	
C2	.2	3.11	80	345	1.66	
D2	1.25A	2.93	345	80	.75	
C4	.2	3.09	80	340	1.67	
D4	.5	3.11	340	75	.75	
C5	.2	3.20	75	350	1.65	Open Circuit For 48 Hours
D5	.5	2.72	305	70	.75	
C6	.25	2.7			1.7	
D6	2	2.4			1.0	
C7	.25	2.7			1.8	
D7	2	2.4			1.0	
C8	.25	2.7			1.8	
D8	2	2.4			1.0	
C9	.25	2.7			1.8	
D9	2	2.4			1.0	
C10	.25	2.7			1.8	
D10	2	3.0			.75	

TABLE IXX

Test Results of Cell #007

Cycle	Current (Amps)	Capacity (Ah)	Pressure (Start) (psi)	Pressure (Finish) (psi)	End Voltage (volts)	Comments
C1	.1	4.69	50	310	1.60	
D1	.5	2.74	310	60	.75	
C2	.2	3.20	60	345	1.76	
D2	2A	2.80	345	85	.60	
C3	.2 A	3.20	80	370	1.75	
D3	1.25A	3.12	370	80	.75	
C4	.2	3.12	80	375	1.76	
D4	.5	3.07	375	60	.75	
C5	.2	3.12	60	340	1.64	
D5	.5	3.06	310	60	.75	Open Circuit For 48 Hours
C6	.25	2.7			1.70	
D6	2	2.4			1.05	
C7	.25	2.7			1.70	
D7	2	2.4			1.05	
C8	.25	2.7			1.70	
D8	2	2.4			1.05	
C9	.25	2.7			1.70	
D9	2	2.4			1.05	
C10	.25	2.7			1.70	
D10	2	3.0			.75	

TABLE IX
Test Results of Cell #008

Cycle	Current (Amps)	Capacity (Ah)	Pressure (Start) (psi)	Pressure (Finish) (psi)	End Voltage (volts)	Comments
C1	.1	4.69	50	290	1.25	
D1	.5	2.79	290	60	.75	
C2	.2	3.20	60	310	1.74	
D2	2 A	2.80	310	75	.70	
C3	.2	3.20	75	340	1.76	
D3	1.25	3.12	340	70	.75	
C4	.2	3.12	70	340	1.76	
D4	.5	3.07	340	50	.75	
C5	.2	3.12	50	300	1.72	Open Circuit For 48 Hours
D5	.5	2.72	275	60	.75	
C6	.25	2.7			1.80	
D6	2 A	2.40			1.0	
C7	.25	2.7			1.80	
D7	2	2.40			1.0	
C8	.25	2.7			1.80	
D8	2	2.40			1.0	
C9	.25	2.7			1.80	
D9	2	2.40			1.0	
C10	.25	2.7			1.80	
D10	2	3.0			.75	

TABLE X
Test Results of Cell #009

Cycle	Current (Amps)	Capacity (Ah)	Pressure (Start) (psi)	Pressure (Finish) (psi)	End Voltage (volts)	Comments
C1	.1	4.8	50	335	1.70	
D1	.5	3.06	335	60	.75	
C2	.2	3.21	60	355	1.71	
D2	2	2.90	355	100	.75	
C3	.2	3.21	100	375	1.75	
D3	1.25	3.06	375	75	.75	
C4	.2	3.21	75	365	1.75	
D4	.5	3.10	365	70	.75	
C5	.2	3.2	70	320	1.64	Open Circuit For 168 Hours
D5	1.25	2.3	280	60	.75	
C6	.25				1.75	
D6	2	2.40			1.02	
C7	.25	2.70			1.75	
D7	2	2.40			1.02	
C8	.25	2.70			1.80	
D8	2	2.40			1.08	
C9	.25	2.70			1.75	
D9	2	2.40			1.02	
C10	.25	2.70			1.75	
D10	2	2.80			.74	

TABLE XI

Test Results of Cell #010

Cycle	Current (Amps)	Capacity (Ah)	Pressure (Start) (psi)	Pressure (Finish) (psi)	End Voltage (volts)	Comments
C1	.1	4.8	50	310	1.70	
D1	.5	2.0	310	110	.75	
C2	.2	3.2	110	355	1.74	
D2	2	2.40	355	155	.75	Short Developed

FIGURE 2 TEST RESULTS OF CELL #009

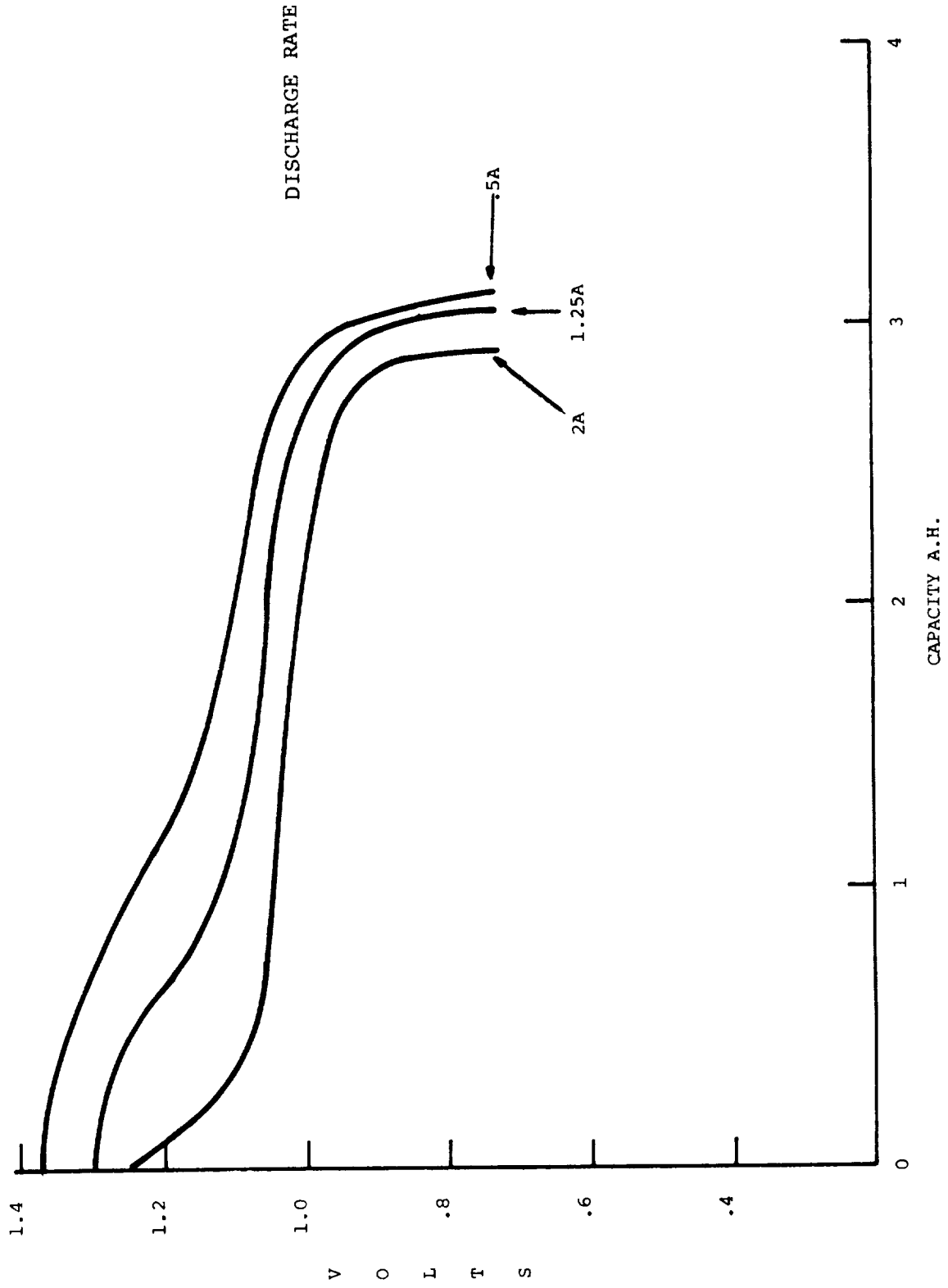


TABLE XII
Test Results of Cell #011

Cycle	Current (Amps)	Capacity (Ah)	Pressure (Start) (psi)	Pressure (Finish) (psi)	End Voltage (volts)	Comments
C1	200mA	9.6	0	360	1.76	Cell leaked repair filled 600
D1	1 A	6.1	600	80	.75	
D1	1 A	6.1	600	80	.75	
C2	400mA	6.5	80	595	1.82	started at 4 Amps
D2	2 A		595	160	.75	
C3	400mA	6.4	160	650	1.83	
D3	1.25	7.9	650	50	.75	Open Circuit for 72 Hours
C4	400mA	6.8	50	595	1.82	
D4	2 A	4.4	490	110	.75	
C5	250mA	2.7			1.70	
D5	2 A	2.4			.90	
C6	.250	2.7			1.70	
D6	2	2.4			.90	
C7	.250	2.7			1.70	
D7	2	2.4			.85	
C8	.250	2.7			1.70	
D8	2	2.4			.95	
C9	.250	2.7			1.70	
D9	2	4.2			.75	

TABLE XIII

Test Results of Cell #012

Cycle	Current (Amps)	Capacity (Ah)	Pressure (Start) (psi)	Pressure (Finish) (psi)	End Voltage (volts)	Comments
C1	200mA	9.6	0	650	1.76	
D1	1 A	6.78	650	50	.75	
C2	400mA	6.2	50	590	1.81	
D2	2 A		590	140	.75	Started at 4 Amps
C3	400mA	6.4	140	660	1.83	
D3	1.25A	7.7	660	90	.75	
C4	400mA	6.8	90	650	1.82	Open Circuit for 72 Hours
D4	2A	4.4	520	130	.75	
C5	250mA	2.7			1.65	
D5	2 A	2.4			.80	
C6	250mA	2.7			1.65	
D6	2 A	2.4			.80	
C7	250mA	2.7			1.65	
D7	2 A	2.4			.80	
C8	250mA	2.7			1.65	
D8	2 A	2.4			.80	
C9	250mA	2.7			1.65	
D9	2 A	4.1			.80	

silver electrodes may be useful for lower rate batteries requiring discharge durations above the 3 hour rate but would not be useful for the synchronous mission (1.2 hour discharge).

Cells 013 and 014 had .125cm (.050") and .124cm (.049") thick silver electrodes. The results of these cells are shown in Tables XIV and XV. Here too, the operating voltages were low at the high current but the capacity utilizations were acceptable.

Cells 015 and 016 contained .063cm (25 mil) silver electrodes. The cells performed normally as shown in Table XVI and were the last in the series in electrode thickness studies.

Based on the results obtained for the silver electrode thickness, an analysis was made to select a silver thickness for the final cell design and further variable testing. The key factor that distinguished the silver electrode thickness results was operating current density which had a substantial effect on the cell voltage. Figure 3 shows the typical voltage, current characteristics of the silver-hydrogen cell. From an analysis of cell weight and operating voltage, the maximum energy density is obtained in a current density range between 35 and 45 mA/sq cm. Since the resultant cell energy density is relatively flat in this range, it was decided to select the lower operating current which will favor the thermal and life characteristics of the cell. Therefore, for a 1.2hr. discharge regimen, the 20Ahr cell design will incorporate 10 silver electrodes each silver electrode nominally .076cm (.030") thick. Each electrode will be of a disk shape previously used to fit into a 6.35cm (2 1/2") diameter cyclinder.

Cells 017 and 018 were the first cells built with the .076cm (.030") silver electrodes. Some difficulty was encountered in initially filling the cells due to a poor vacuum apparatus and they exhibited initially poor performance. The testing was discontinued and the same variables were later rebuilt.

Cells 019 and 020 also contained the .076cm (.030") nominal silver electrode, but were built without any electrolyte reservoir. In the place of the electrolyte reservoir was a polypropylene plastic gas diffusion screen to allow hydrogen access to the back-side of the fuel cell electrodes. The results of these cells were similar to cells without the reservoirs and showed very good performance. Figure 4 shows the family of discharge curves at different rates for cell 020. Based on the promising results of cells 019 and 020, cell 021 was built with 2 silver electrodes stacked in parallel to initiate the studies of multi electrode constructions.

TABLE XIV

Test Results of Cell #013

Cycle	Current (Amps)	Capacity (Ah)	Pressure (Start) (psi)	Pressure (Finish) (psi)	End Voltage (volts)	Comments
C1	.15	7.9	0	500	1.72	
D1	.75	4.9	500	70	.75	
C2	.3	4.8	70	485	1.76	
D2	3	3.75	485	110	.75	
C3	.3	4.8	110	515	.78	
D3	1.80	4.7	515	100	.75	

TABLE XV

Test Results of Cell #014

Cycle	Current (Amps)	Capacity (Ah)	Pressure (Start) (psi)	Pressure (Finish) (psi)	End Voltage (volts)	Comments
C1	.15	7.9	0	470	1.72	
D1	.75	4.66	470	60	.75	
C2	.3	4.8	60	475	1.72	
D2	3	3.3	475	180	.75	
C3	.3	4.8	180	510	1.85	
D3	1.80	4.2	510	150	.75	

TABLE XVI
TEST RESULTS OF CELL #015 and 016

Cycle	Current	#015				#016			
		Ahr	P ₁	P ₂	V	Ahr	P ₁	P ₂	V
C1	.1	3.5	50	300	1.70	3.5	50	290	1.70
D1	.5	2.8	300	60	.75	2.6	290	50	.75
C2	.2	3.0	60	300	1.75	3.0	50	300	1.75
D2	2	2.6	300	70	.75	2.5	300	80	.75
C3	.2	3.0	70	300	1.75	3.0	80	300	1.75
D3	1.2	2.6	300	75	.75	2.5	300	75	.75
C4	.2	3.0	75	310	1.75	3.0	75	305	1.75
D4	.5	2.7	310	70	.75	2.6	305	75	.75
C5	.2	3.0	70	310	1.75	3.0	75	300	1.75
D5	1.2	2.0	260	60	.75	2.0	240	55	.75
C6	.2	3.0			1.75	3.0			1.75
D6	1.8	2.1			1.02	2.1			1.02
C7	.2	2.4			1.75	2.4			1.75
D7	1.8	2.1			1.02	2.1			1.02
C8	.2	2.4			1.75	2.4			1.75
D8	1.8	2.1			1.02	2.1			1.02
C9	.2	2.4			1.75	2.4			1.75
D9	1.8	2.1			1.02	2.1			1.02
C10	.2	2.4			1.75	2.4			1.75
D10	1.8	2.5			.75	2.4			.75

FIGURE 3 SILVER-HYDROGEN POLARIZATION

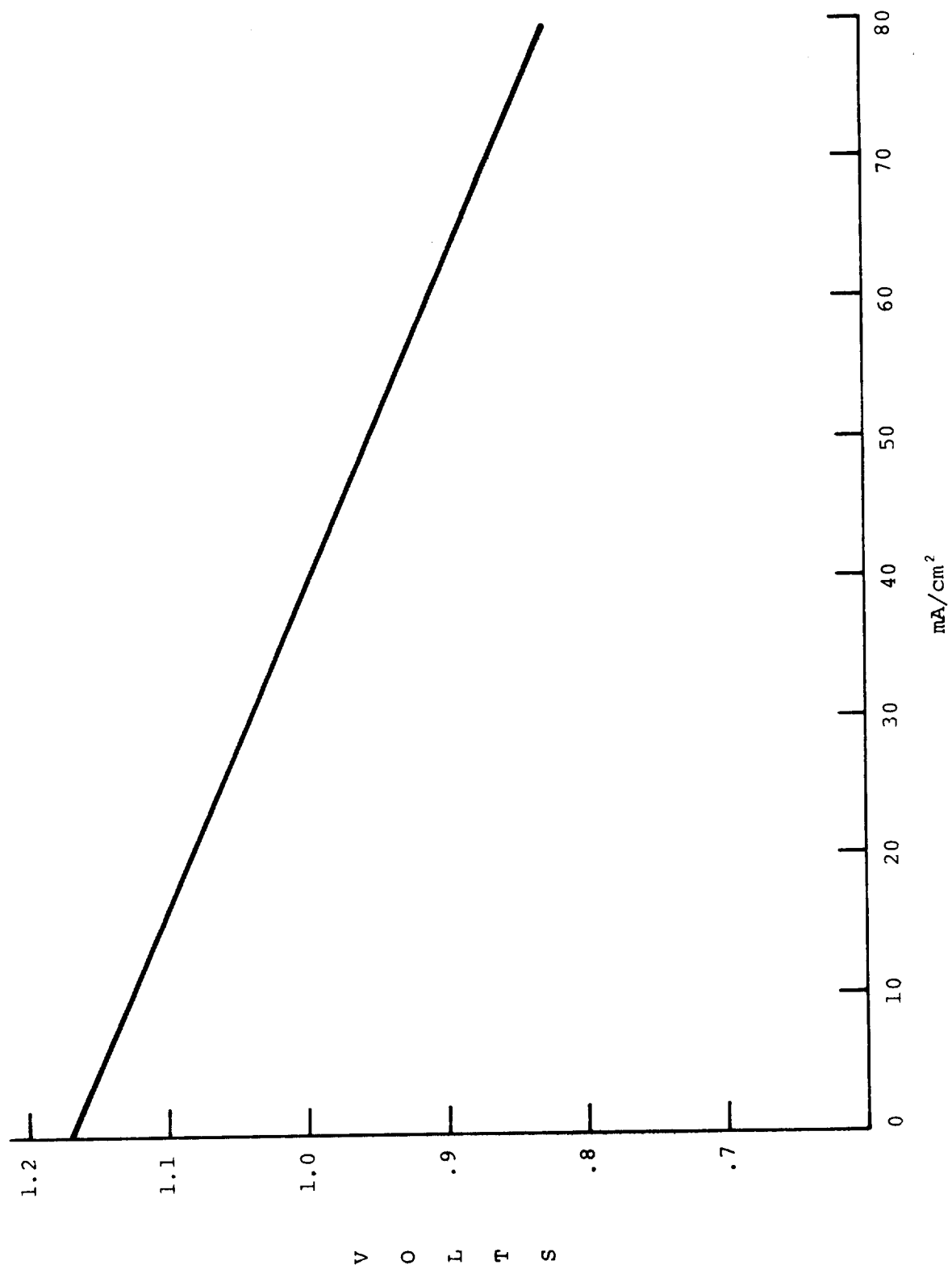
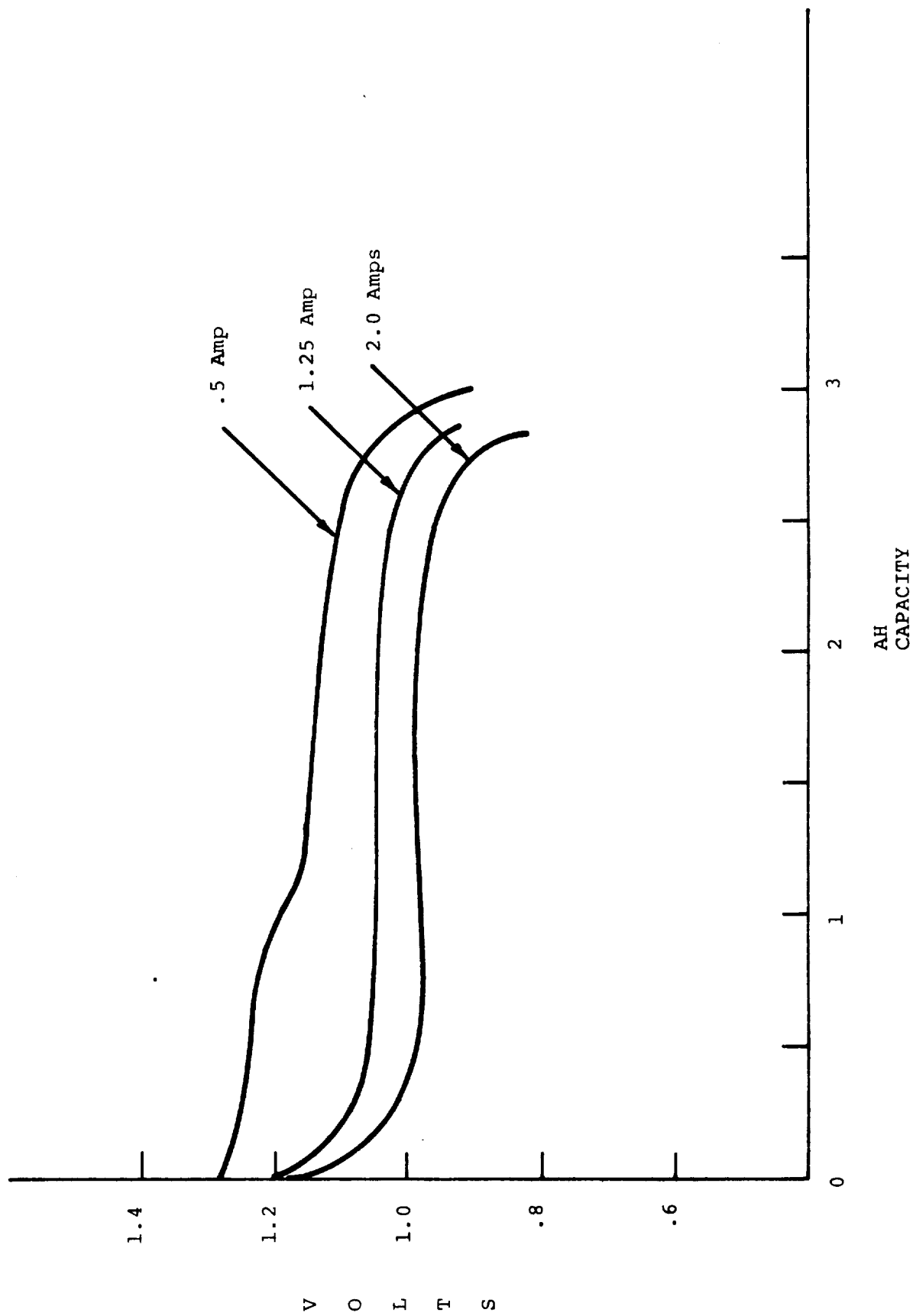


FIGURE 4 CELL #20 PERFORMANCE



This assembly was put together to evaluate any complications in multi-electrode stacking. The cell was subjected to a series of electrical tests at twice the currents normally used for a single electrode cell. The results were acceptable as shown in Table XVII however, the operating voltage was found to be 50 - 100 milli volts lower than anticipated. A review of the construction showed that the insulated feedthroughs in the test housing were inadequate to carry the test currents and high IR drops were observed. Accounting for the IR drops the operating performance was considered normal and the testing was discontinued to use the boiler-plate for other test cells. Cells 022 and 023 consisted of .076cm (30 mil) silver electrodes and the (.056cm) (22 mil) electrolyte reservoirs for further comparison and verification testing of the .076cm silver electrode with the reservoir. These cells were put through the entire test sequence and showed stable performance similar to previously observed as shown in Table XVIII. Since in the initial cycling of the cells it is not possible to determine effects of electrolyte reservoir on the cell performance, it was decided not to continue the electrolyte reservoir tests.

The next series of cell tests was directed at electrolyte concentration studies. Cells 024, 025, 028, 029, 030, and 031 were put through the standard test regime consisting of discharges at a .5 amps, 1.60 amps and 2 amps. Based on the initial test results, there was no substantial difference in the operating voltage or the capacity output from the cells as shown in Table XIX. This result was somewhat surprising, but apparently with the quantity of electrolyte employed, the cell size and test condition we were not in a limiting range.

There are conflicting considerations in selecting the optimum electrolyte concentration. Lower concentration KOH is favored since it contains a larger fraction of water and therefore, is less subject to concentration changes. From a thermal standpoint, the higher KOH concentration is favored because this has a lower vapor pressure and minimizes potential water condensation problems in the cell. From a conductivity standpoint, 33% electrolyte is the most conductive. On the basis of the testing done and silver-zinc battery history, the greatest amount of experience exists with 30 to 35% KOH. Therefore, in the absence of any other input, we selected 30% KOH electrolyte to be used in the final cells.

Cells 026 and 027 contain 30% electrolyte and they were constructed to analyze the contribution that the electrolyte reservoir makes to the cell. The cells were assembled, filled in the normal manner and given one charge and rapidly disassembled and the electrolyte reservoirs were removed from the cell and the KOH concentration was analyzed. A problem occurred in the analysis of the IER from cell 026 and no results were obtained. For cell 027 the electrolyte concentration was determined by titration to be 36% which means that the electrolyte reservoir was contributing a significant

TABLE XVII
TEST RESULTS OF CELLS #021

Cycle	Current (Amps)	Capacity (Ahr)	Pressure (Start) (psi)	Pressure (Finish) (psi)	End Voltage (Volts)	Comments
C1	.15	7	0	460	1.7	
D1	1	4.8	480	25	.5	
C2	.3	5.0	25	500	1.75	
D2	2	4.8	500	40	.5	
C3	.3	5.0	40	490	1.75	
D3	2.5	4.4	490	60	.5	
C4	.3	5.0	60	490	1.75	
D4	1	4.5	490	50	.5	

TABLE XVIII
TEST RESULTS OF CELLS #022 and 023

Cycle	Current	Ahr	Cell 022			Cell 023			
			P ₁	P ₂	V	Ahr	P ₁	P ₂	V
C1	.1	3.5	50	300	1.70	3.5	50	305	1.70
D1	.5	2.9	300	50	.75	2.9	305	50	.75
C2	.2	3.0	50	310	1.75	3.0	50	310	1.75
D2	2	2.3	310	70	.75	2.4	310	60	.75
C3	.2	3.0	70	300	1.75	3.0	60	300	1.75
D3	1.6	2.5	300	60	.75	2.5	300	50	.75
C4	.2	3.0	60	310	1.75	3.0	50	320	1.75
D4	.5	2.6	310	75	.75	2.5	320	70	.75
C5	.2	3.0	75	315	1.75	3.0	70	310	1.75
D5	1.6	1.7	260	50	.75	1.8	280	55	.75
C6	.22	2.2			1.75				
D6	1.6	2.0			1.04				
C7	.22	2.2			1.75				
D7	1.6	2.0			1.03				
C8	.22	2.2			1.75				
D8	1.6	2.0			1.03				
C9	.22	2.2			1.75				
D9	1.6	2.0			1.03				
C10	.22	2.2			1.75				
D10	1.6	2.5			.75				

TABLE XIX

TEST RESULTS OF CELLS #024, 025, 028, 029, 030, 031

Cycle #	Current	#024		#025		#028		#029		#030		#031	
		Ahr	V	Ahr	V	Ahr	V	Ahr	V	Ahr	V	Ahr	V
C1	.1	3.5	1.70	3.5	1.70	3.5	1.70	3.5	1.70	3.5	1.70	3.5	1.70
D1	.5	2.9	.75	2.9	.75	2.8	.75	2.7	.75	2.9	.75	2.8	.75
C2	.2	3.0	1.75	3.0	1.75	3.0	1.75	3.0	1.75	3.0	1.75	3.0	1.75
D2	2	2.3	.75	2.5	.75	2.7	.75	2.6	.75	2.6	.75	2.6	.75
C3	.2	3.0	1.75	3.0	1.75	3.0	1.75	3.0	1.75	3.0	1.75	3.0	1.75
D3	1.6	2.5	.75	2.5	.75	2.4	.75	2.6	.75	2.5	.75	2.7	.75
C4	.2	3.0	1.75	3.0	1.75	3.0	1.75	3.0	1.75	3.0	1.75	3.0	1.75
D4	.5	2.7	.75	2.6	.75	2.5	.75	2.7	.75	2.6	.75	2.6	.75
C5	.2	3.0	1.75	3.0	1.75	3.0	1.75	3.0	1.75	3.0	1.75	3.0	1.75
D5	1.6	2.6	.75	2.4	.75	2.5	.75	2.5	.75	2.4	.75	2.6	.75

4. FINAL DESIGN

Based on the results of single electrode cell tests and other metal-gas experience, a 20Ahr cell design was prepared.

4.1 Cell Description

Figure 5 shows the sectional drawing of the 20Ahr silver-hydrogen cell. The cell housing consists of a cylindrical tube section and two hemispherical domes. In each of the hemispherical caps one insulated feedthrough is provided. In addition, the negative feedthrough provides for a gas access to the cell for purposes of filling the cell with gas and checkout. The electrodes are stacked between two plastic endplates and are anchored to the cell housing by means of four tierods. The void volume within the cell housing is sized to accommodate the desired operating pressure for the cell's rated capacity. The electrode stack consists of a repeating sequence of layers as shown in Figure 6 consisting of the electrolyte reservoir, hydrogen electrode, separator material, silver electrode, separator material, hydrogen electrode, and electrolyte reservoir. Tabs are spot welded to the respective electrodes and brought out the sides of the electrode stack. These tabs are then connected to the respective terminal rods by means of silver brazing. The electrode stack tierods are anchored by means of spot welding to the two ends of the cell housing. The assembly sequence is as follows:

1. The electrodes in their proper sequence are stacked between the endplates and tierods.
2. The tierods are tightened on the stack to the desired stack height.
3. The respective positive and negative tabs are bent and groomed to fit along the electrode stack.
4. The terminal rods are brazed to the stack tabs.
5. The electrode stack is assembled in the cylindrical section of the housing and the anchoring tabs are spot welded to the ends of the cylindrical housing.
6. The domes are fitted to both sides of the cell housing.
7. The compression fittings are welded into the domes and the domes are welded onto the tubes.
8. The cell assembly is proof and leak tested.

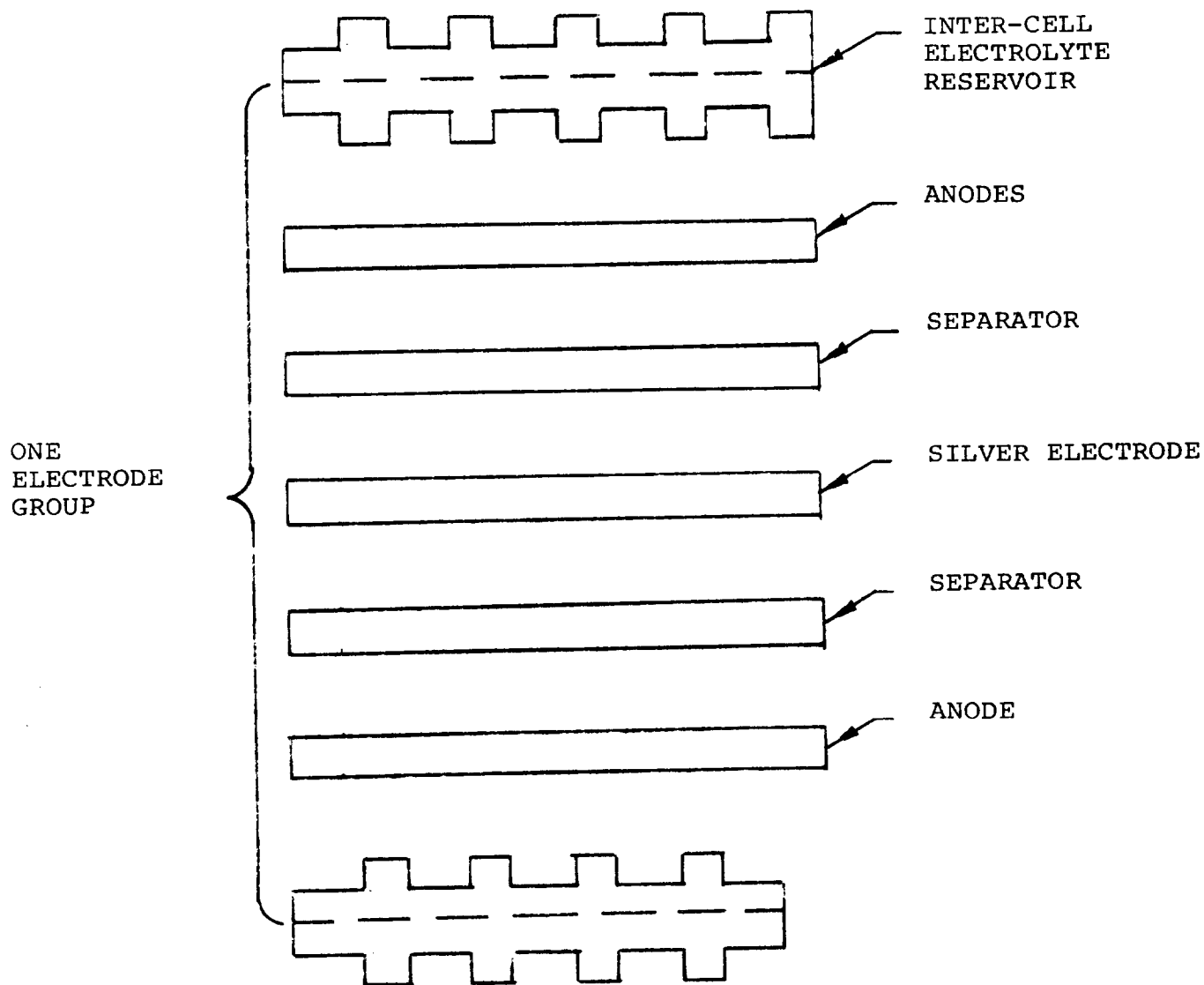


FIGURE 5 AgO-H₂ STACK SEQUENCE

9. The cell assembly is back filled by means of vacuum with excess electrolyte.
10. The assembly is given a soak period of 16 hours at 80°C.
11. The excess electrolyte is drained from the cell.
12. The cell is put on a formation charge at .7 amps for 50 hours.
13. The cell is backed filled with hydrogen to 3,447KN/m² (500 psi) and subjected to the first discharge at 5 amps to a .75 volt endpoint.

4.2 Electrode Stack

The following sections describe the design and fabrication by doctoring a fine silver powder, Handy and Harmon all powder number 130, onto a moving belt to a desired height. Silver expanded metal (5Ag 5 4/0) is fed into the silver powder layer which is then sent through a set of calender rollers. The rollers compact the silver powder to the desired electrode density. The compacted silver powder, and silver expanded metal have sufficient strength to be handled. This strip is placed in a preheated sintering furnace which is maintained at 650°C for a two minute period. The sintering process bonds the grid and the silver particles together to provide the desired structural integrity. The strip is then die cut into the appropriate size electrode. The porosity reproducibly achievable by this process and sil power #130 is (apparent density of 3.8 grams per cc) 63.8% and this is the design porosity. Figure 7 shows the electrode size.

Separator Edge Seal

In the stack disc configuration it is necessary to provide some sort of edge protection. If the silver electrode, separators and the hydrogen electrode are sized to the same outside diameter, there is a possibility of shorting caused by whiskers at the edges of the electrodes and there is a potential silver migration path around the edge of the separator material. Therefore, some edge sealing or masking is required. The final design approach is to extend the diameter of the separator material .16cm (1/16") beyond the diameter of the electrode and this will prevent the shorting problem and appears to be sufficient to minimize soluble silver from bridging around the edge of the separator.

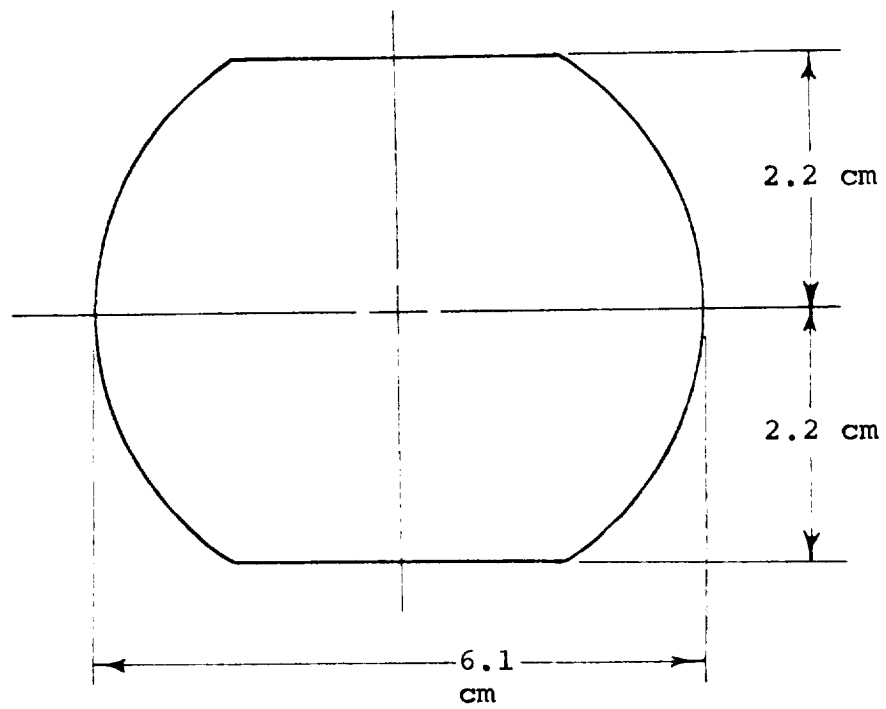


FIGURE 7

ELECTRODE SHAPE

Intercell Electrolyte Reservoirs

The IER are fabricated from Carbonyl nickel powders Inco number 287. This enables the fabrication of a sintered porous plaque that has the desirable mechanical integrity and a pore size distribution in the 1 to 10 micron range at 80% porosity.

The hydrogen flow field is shown in Figure 8. This provides for a hydrogen flow field depth and width of .17mm and a ϕ of .64. To fabricate the IER's, a flat sheet of porous nickel is sintered. The flow field is then coined into the sheet by pressing a (8 x 8 x .017cm) (20 x 20 x .007") screen into each face with a pressing die.

4.3 Cell Hardware

Pressure Shell

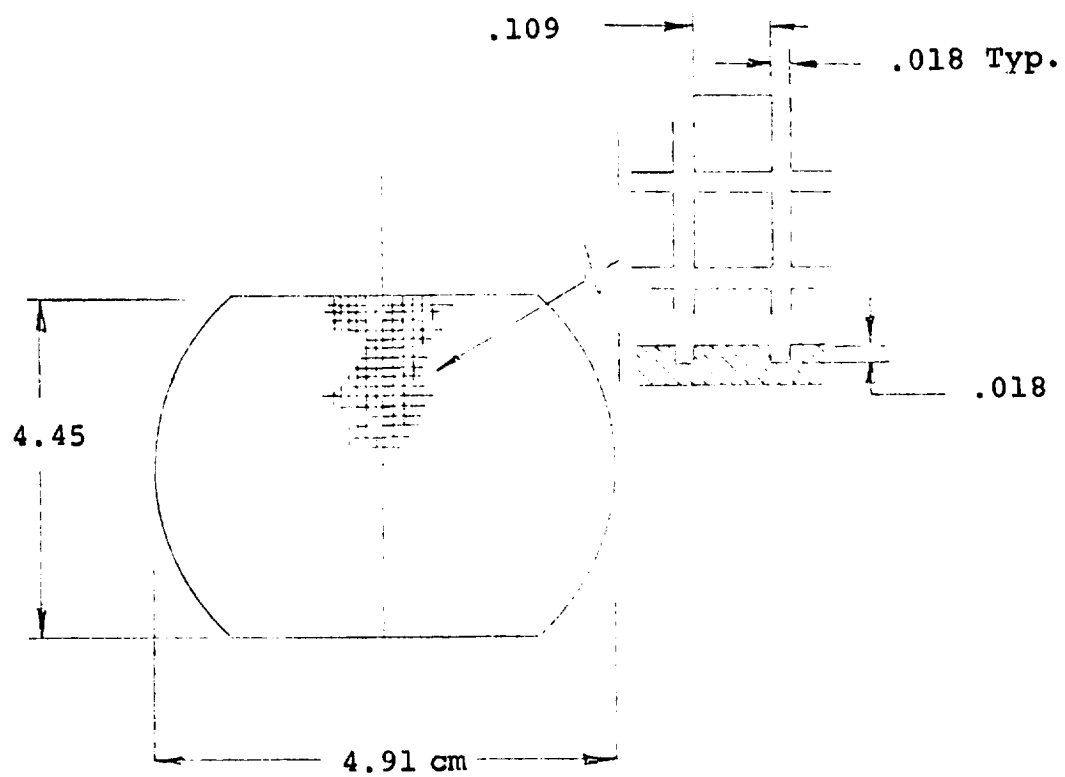
The pressure shell will be fabricated from Inconel 718. The vessel has a nominally 6.35cm (2.5") diameter. The choice of Inconel 718 material has been made on the basis of the following features:

1. The material is high strength, yield strength of 1,034MN/m² (150,000 psi) with an ultimate strength of 1,241MN/m² (180,000 psi).
2. The can can be readily fabricated in thin walls of type necessary to make a lightweight vessel.
3. The Inconel is chemically stable and does not exhibit any substantial hydrogen diffusion.

The minimum design criteria for the vessel is an operating pressure of 3,447KN/m² (500 spi) a proof pressure of 1 1/2 times the operating, and a burst pressure 2 times the operating pressure. However, due to material availability and weldability, a greater wall thickness is utilized and the housing will have a 2.9 safety factor to burst.

Terminals

The terminals are a plastic type compression seal sometimes referred to as the Ziegler seal. The seal consists of an outer metal busing (Inconel) that has an internal thread in it. A plug of plastic is molded into the busing to fill all the voids and conforming exactly to the thread that is cut in the bushing. A hole is then reamed in the center of the plastic to form a tight fit to the terminal rod which is inserted in the hole. The outer barrel



NOTE:

$$\alpha = .64$$

FIGURE 8 INTER-CELL ELECTROLYTE RESERVOIR

is then compressed in a crimping tool. The concept of the seal is by crimping the outer barrel, the plastic material is held in a compressive load in its elastic limit. If the terminal is subjected to thermal expansion and contraction or stresses which cause movement of the outer barrel or a change in diameter of the rod, the plastic compensates for movement and the seal remains intact.

There is some latitude in the choice of the plastic for the seal and the design is based on Kynar which is a high temperature chemically resistant fluorocarbon.

The central terminal rod can be of a variety of materials depending on the cell design. For the 20Ahr seal, the terminal design utilizes a .32cm (1/8") diameter rod. A silver plated copper rod will be utilized to minimize the IR drop for the 20Ahr cell capable of operating at the one hour rate (20 amperes).

Stack Endplates and Tie Rods

To hold the electrode stack in compression two plastic endplates are utilized. The endplates are utilized. The endplates will be fabricated from polysulfone. This material is chemically stable in the AgO-H cells and has a high strength. The endplates are molded with cross ribs to make a lightweight stiff construction. The tie rods for the 20 ampere-hour size cell consist of four .24cm (.093") stainless steel rods. They are threaded on the top and bottom such that the bottom nuts support the endplate in a flat plan across the bottom and the top nuts are utilized to compress the stack. Epoxy is utilized to lock the nut to be stable in vibration.

4.4 Cell Design

Based on the materials and components described in the previous section and the test results obtained in Task II, a final design was prepared. There are a **number** of critical factors that must be established to freeze the **design**. The key operating parameter is the number of electrodes or operating current density. From an analysis of the test results, a current density of 35mA/sq cm is preferred and this was used as the basis. The factors of the design are listed below:

1. Silver Utilization - 3.5 grams per ampere-hour
2. Silver Density - 3.8 grams per cc
3. Electrode number - 10

4. Operating Pressure Range - 689-3,447KN/m² (100 to 500 psi)
(for 20Ahr)
5. Starting Electrolyte Concentration 30% KOH
6. Pressure Vessel Diameter 6.35cm (2.4")
7. Electrolyte Reservoir F = .5 Total, Volume 14 cc

The quantity of hydrogen required for a 20Ahr capacity is (20) .0376 gm/Ahr = .752 gm. A decision is made that the 20Ahr will be achieved over 689 3,447KN/m (100-500 psi), therefore the vessel requires a total of .94 g of hydrogen. The volume of hydrogen taking into account the compressibility is determined by:

$$V_{H_2} = \frac{Z}{P} \times \frac{22,428}{2.0154} (W_{H_2}) \text{ where;}$$

$$V_{H_2} = H_2 \text{ volume}$$

$$Z = \text{compressibility factor (1.095)}$$

$$P = \text{pressure}$$

$$W_{H_2} = \text{weight of hydrogen}$$

From the compressibility data of hydrogen at 20°C, the storage volume for hydrogen required is 330.5cm³ (20.15in³). For a 20 ampere-hour cell the displaced volume; which includes the electrolyte, which is absorbed in the electrodes and separator is shown in Table XX.

Utilizing the displaced volume of 85.2cm³ (5.2 in³) and the hydrogen volume of 330.5cm³ (20.15in³) the pressure vessel volume is 415.7cm³ (25.35in³). The cylinders design is based on an arrangement of hemispherical caps on a cylindrical tube. For the selected 6.35cm (2.5") diameter vessel, the cylinder length is 9.2cm (3.6 in.). The thickness of the pressure shell was determined on the basis of the thin wall pressure vessel theory and a yield stress of 92,500 psi as shown in Table XXI. The weight was determined on the basis of an Inconel 718 density 8.2gm/cc (.296 lb/in³). The cylinder design is based on the dome thickness being to the cylindrical shell thickness. Table XXII also shows a weight breakdown of the cylindrical section and the domes.

Table XXIII shows the design of the IER based on the flow field as presented in Figure 8. Table XXIV shows the design and weight breakdown of the 20Ahr cell.

TABLE XX
PRESSURE VESSEL SIZING

Stack Height

	<u>Thickness / Number</u>			
	(cm)			
Silver	.076	x	10	.76
Separator	.040	x	20	.81
IER	.055	x	11	.61
Hydrogen Electrode	.013	x	20	.25
End Plate	.24	x	2	<u>.48</u>
				2.91 cm
Stack Displacement	2.94 x 24.8	=		72.1 cm ³
Miscellaneous				<u>13.1 cm³</u>
				85.2 cm ³
Pressure Vessel Volume	85.2 + 330.5 = 415.9 cm ³			
Sphere Volume	6.32 Diameter 132.5 cm ³			
Cylinder Length	$\frac{415.7 - 132.5}{30.64} = 9.2 \text{ cm}$			

TABLE XXI
PRESSURE VESSEL DESIGN AND
WEIGHT BREAKDOWN

Inconel 718 - Tensile Strength 1,241 MN/m² (180,000 psi)
Yield Strength
(.2% offset) 1,032 MN/m² (150,000 psi)

$$\text{Design Limit } \frac{1,241}{2} = 621 \text{ MN/m}^2$$

$$\text{or, } \frac{1,032}{1.5} = 688 \text{ MN/m}^2$$

$$t = \frac{PD}{2S} = \frac{3.44 \cdot 6.35}{621 \cdot (2)} = .017 \text{ cm}$$

use .025 cm due to material availability and weldability

Cylinder Weight

$$6.35 \pi (.025) (9.22) (8.2) = 38 \text{ gms}$$

Dome Weight

$$4 \pi (3.175)^2 (.025) (8.2) = 27$$

Weld Ring

$$\pi 6.35 \times .025 \times 1.27 (8.2) \quad \underline{6}$$

TOTAL 71 gms

TABLE XXII
INTER-CELL ELECTROLYTE RESERVOIR DESIGN

$$d = \frac{.34C''}{\epsilon(1-F)} = 2\delta [1-\alpha]$$

where

δ = .007 in., .0039cm (flow field depth)

A = 10 (3.85)" = 38.5in, 248.3 cm (Cell area)

α = .64 (Area in contact with anode/total area)

C = 20 (Cell capacity)

$C'' = \frac{20}{248.3} = .08$ (Capacity/unit area)

ϵ = .8 (Reservoir porosity)

F = .5 (Design factor, fraction of reservoir filled)

d = .06 cm, .024 inches (Reservoir thickness)
=

Reservoir Volume = cc 14 cc

Reservoir Weight = 30 gms.

TABLE XXIII
DESIGN AND WEIGHT BREAKDOWN OF
20 Ahr Ag-H₂ CELL

Component	Unit Wt.	Quantity	Weight (gms)	Total (gms)
Silver Electrode	3.5gm/Ahr	10	7.00	70
Silver Grid	.04gm/cm ²	10	1.03	10
Silver Wire		10	.4	4
Astropower Separator	.06gm/cm ²	20	1.60	32
Hydrogen Electrode	.04gm/cm ²	20	1.0	20
Nickel Wire		20	.5	10
Electrolyte Reservoir		11	2.7	30
End Plates		2	9.1	18
Tie Rod		4	3	<u>12</u>
Total Stack				206
Pressure Vessel				71
Seals & Terminals				15
Electrolyte		10 x	5.0	50
Miscellaneous				<u>15</u>
Total				357 gms (.785 lbs)

$$\text{Estimated Energy Density} = \frac{1.05 (20)}{.357} = 58.7 \text{Wh/Kgm (26.7Whr/lb.)}$$

Volume

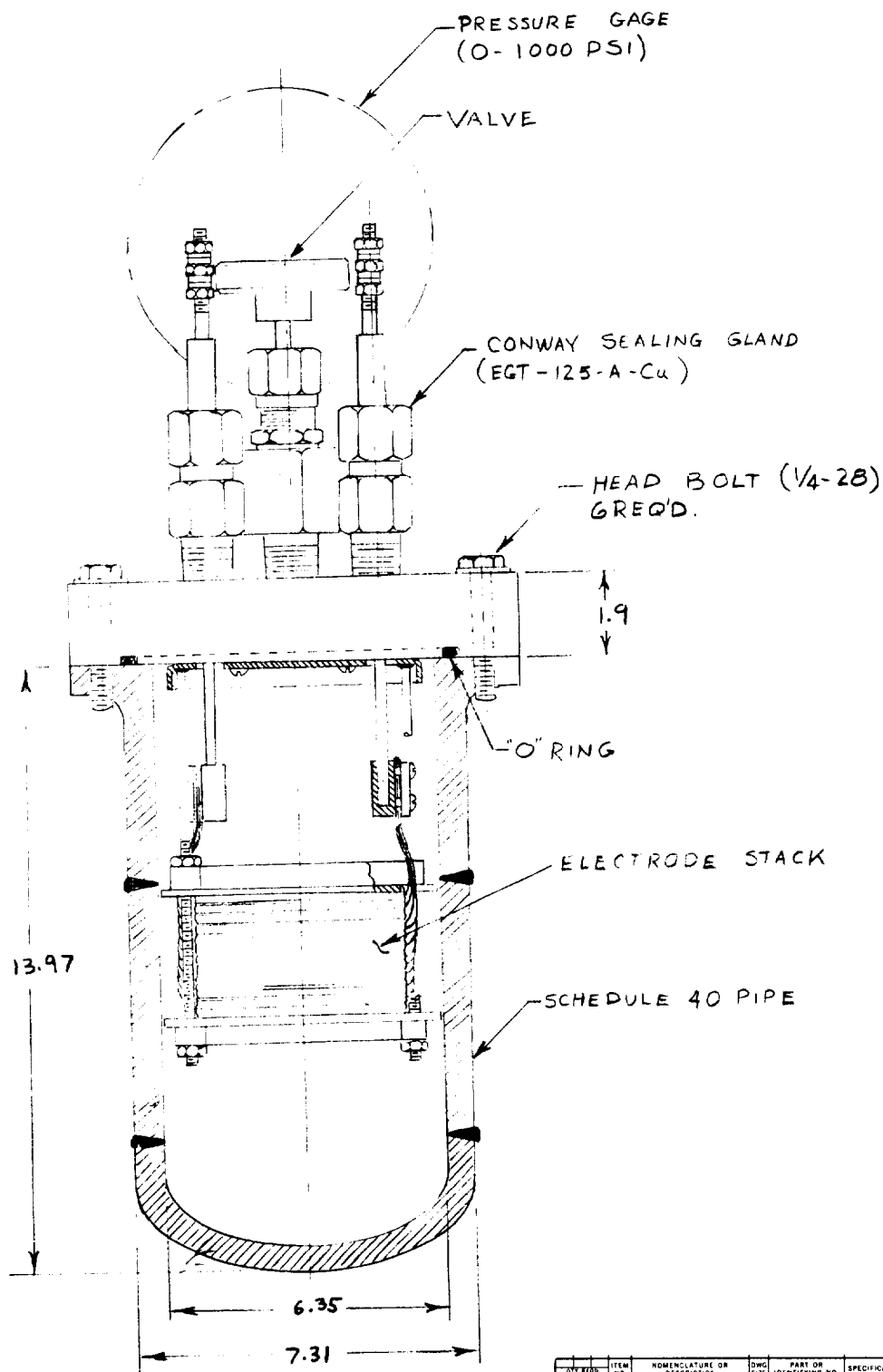
Actual 426 cm³ (26in³)

$$\text{Estimated Energy Density} = \frac{1.05 (20)}{426} = .05 \text{Whr/cm}^3 \text{ (.8Whr/in}^3\text{)}$$

5. DESIGN, FABRICATION AND TEST OF 20Ahr CELLS

The design and fabrication of four heavy wall housings to accomodate 20Ahr electrode stacks was undertaken. Figure 9 shows a sectional drawing of the 20Ahr assembly. The electrode stack employed was of the same design and construction that would be utilized in a lightweight cell with the exception that positive and negative tabs come out the top of the cell and the lightweight design cells for terminals out opposite ends of the cell. The internal free volume within the heavy wall housing was sized for the cell to operate over a pressure range of 689-3447kN/m² (100 to 500psi). Figure 10 shows a photograph of the electrode stack and Figure 11 shows the assembly.

The cells were assembled and subjected to five acceptance cycles, the data of which is presented in Tables XXIV through XXXIII.



SYMBOL FOR DATA	ITEM NO.	NOMENCLATURE OR DESCRIPTION	DWG SIZE	PART OR IDENTIFYING NO.	SPECIFICATION	MATERIAL OR NOTE	REMARKS
LIST OF MATERIAL							
UNLESS OTHERWISE SPECIFIED DIMENSIONS ARE IN INCHES FRACTIONS DECIMALS ALL SURFACES UNLESS OTHERWISE SPECIFIED SHALL BE TO FINISH HOLE LOCATIONS SHALL BE TO CENTER DIMENSIONS TO SURFACE UNLESS OTHERWISE SPECIFIED		ENERGY RESEARCH CORPORATION					
MATERIAL		C					
FINISH		C					
APPLICATION		C					

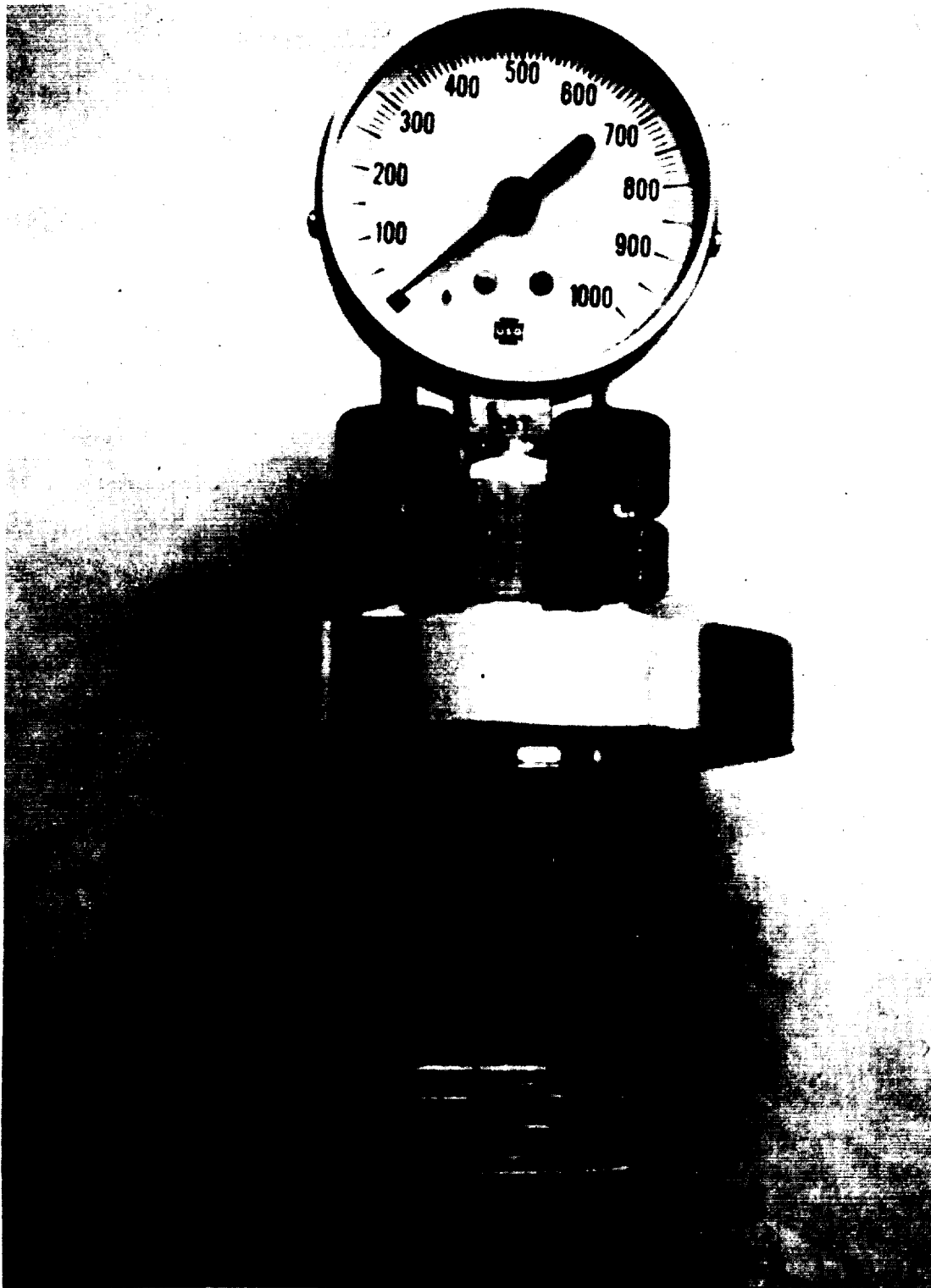


FIGURE 10 20Ahr ELECTRODE STACK

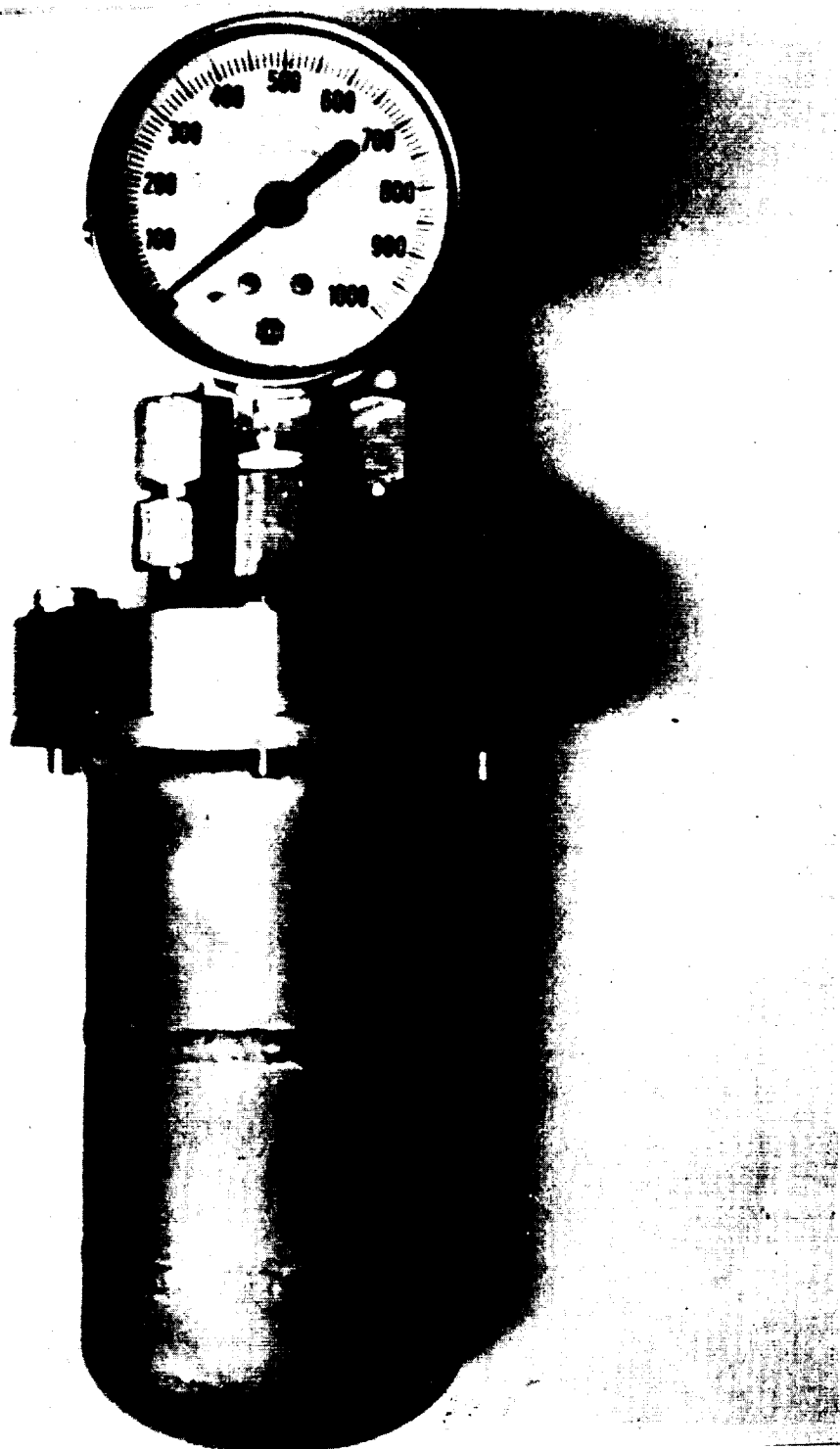


FIGURE 11 HEAVY HOUSING ASSEMBLY

TABLE XXIV

CYCLE #1

TIME	I (Ampere)	S/N 2		S/N 4		REMARKS
		V (volts)	P (psi)	V (volts)	P (psi)	
0 Hr	.8	1.15	0	1.14	0	Charge
50	.8	1.70	490	1.71	550	
0 MIN	16.6	1.42	490	1.20	550	Discharge
10	16.6	1.36	450	1.10	485	
20	16.6	1.16	395	1.10	425	
30	16.6	1.10	340	1.10	390	
40	16.6	1.10	280	1.11	325	
50	16.6	1.10	230	1.11	275	
60	16.6	1.10	160	1.10	215	
70	16.6	1.09	100	1.09	130	
72	16.6	1.09	100	1.07	120	

TABLE XXV

CYCLE #2

TIME	I (Ampere)	S/N 2		S/N 4		REMARKS
		V (volts)	P (psi)	V (volts)	P (psi)	
0 HR	1	1.21	100	1.21	120	Charge
22.8	1	1.72	510	1.72	565	
0 MIN	16.6	1.32	510	1.24	565	Discharge
10	16.6	1.16	465	1.09	510	
20	16.6	1.10	400	1.10	450	
30	16.6	1.11	350	1.10	400	
40	16.6	1.11	285	1.10	340	
50	16.6	1.10	245	1.09	290	
60	16.6	1.10	170	1.09	225	
70	16.6	1.07	165	1.08	155	
72	16.6	1.06	95	1.08	150	

TABLE XXVI

CYCLE #3

TIME		I (Ampere)	S/N 2		S/N 2		REMARKS
			V (volts)	P (psi)	V (volts)	P (psi)	
0	HR	1	1.21	87	1.21	140	Charge
22.8		1	1.72	512	1.72	555	
0	MIN	16.6	1.30	512	1.29	555	Discharge
10		16.6	1.09	455	1.07	490	
20		16.6	1.10	390	1.08	430	
30		16.6	1.10	350	1.08	395	
40		16.6	1.10	285	1.08	330	
50		16.6	1.10	240	1.08	280	
60		16.6	1.09	180	1.07	220	
70		16.6	1.07	115	1.06	150	
72		16.6	1.06	110	1.06	150	

TABLE XXVII

CYCLE #4

TIME		I (Ampere)	S/N 2		S/N 4		Remarks
			V (volts)	P (psi)	V (volts)	P (psi)	
0	HR	1	1.21	110	1.21	150	Charge
22.8		1	1.73	520	1.72	560	
0	MIN	16.6	1.29	520	1.28	560	Discharge
10		16.6	1.08	470	1.07	505	
20		16.6	1.09	415	1.08	445	
30		16.6	1.10	360	1.09	400	
40		16.6	1.10	300	1.09	345	
50		16.6	1.10	250	1.09	290	
60		16.6	1.09	180	1.08	225	
70		16.6	1.08	115	1.07	150	
72		16.6	1.05	110	1.07	150	

TABLE XXVIII

CYCLE #5

		S/N 2		S/N 4			
TIME		I (Ampere)	V (volts)	P (psi)	V (volts)	P (psi)	Remarks
0	HR	1	1.21	110	1.21	150	Charge
22.8		1	1.73	540	1.72	570	
0	MIN	16.6	1.27	540	1.11	570	Discharge
10		16.6	1.13	490	1.09	545	
20		16.6	1.09	430	1.09	470	
30		16.6	1.10	365	1.09	320	
40		16.6	1.10		1.09		
50		16.6	1.11	260	1.09	300	
60		16.6	1.10	200	1.08	240	
70		16.6	1.09	140	1.05	175	
72		16.6	1.06	120	1.03	160	

TABLE XXIX

CYCLE #1

TIME	I (Ampere)	S/N 1		S/N 3		REMARKS
		V (volts)	P (psi)	V (volts)	P (psi)	
0 Hr	.8	1.18	0	1.18	0	Charge
50	.8	1.68	390	1.68	400	
0 MIN	16.6	1.31	390	1.34	400	Discharge
10	16.6	1.28	340	1.24	375	
20	16.6	1.08	240	1.09	320	
30	16.6	1.08	240	1.08	290	
40	16.6	1.07	180	1.08	235	
50	16.6	1.06	130	1.06	170	
60	16.6	1.00	75	1.05	90	
70	16.6	.95	20	.95	40	
72	16.6	.75	10	.75	20	
						Added 100 psi

TABLE XXX

CYCLE #2

TIME	I (Ampere)	S/N 1		S/N 3		REMARKS
		V (volts)	P (psi)	V (volts)	P (psi)	
0 Hr	1	1.21	100	1.21	120	Charge
22.8	1	1.72	540	1.72	565	
0 MIN	16.6	1.34	540	1.33	565	Discharge
10	16.6	1.16	490	1.27	510	
20	16.6	1.04	430	1.09	460	
30	16.6	1.09	350	1.10	400	
40	16.6	1.09	285	1.09	340	
50	16.6	1.08	270	1.09	290	
60	16.6	1.08	220	1.09	245	
70	16.6	.80	165	1.07	180	
72	16.6	.80	155	1.06	170	

TABLE XXXI

CYCLE #3

TIME	I (Ampere)	S/N 1		S/N 3		REMARKS
		V (volts)	P (psi)	V (volts)	P (psi)	
0 HR	1	1.21	155	1.21	170	Charge
22.8	1	1.72	560	1.69	570	
0 MIN	16.6	1.29	560	1.32	570	Discharge
10	16.6	1.07	510	1.21	520	
20	16.6	1.06	450	1.06	465	
30	16.6	1.05	400	1.06	410	
40	16.6	1.06	350	1.07	360	
50	16.6	1.06	300	1.07	310	
60	16.6	1.05	250	1.07	260	
70	16.6	1.03	190	1.06	200	
72	16.6	1.02	180	1.06	185	

TABLE XXXII

CYCLE #4

TIME	I (Ampere)	S/N 1		S/N 3		REMARKS
		V (volts)	P (psi)	V (volts)	P (psi)	
0 HR	1	1.21	180	1.21	185	Charge
22.8	1	1.70	585	1.70	585	
0 MIN	16.6	1.26	585	1.29	585	Discharge
10	16.6	1.06	530	1.15	525	
20	16.6	1.05	475	1.06	475	
30	16.6	1.05	420	1.06	420	
40	16.6	1.06	370	1.07	370	
50	16.6	1.05	310	1.07	310	
60	16.6	1.05	255	1.06	255	
70	16.6	1.02	200	1.05	200	
72	16.6	1.01	185	1.05	180	

TABLE XXXIII

CYCLE #5

TIME	I (Ampere)	S/N 1		S/N 3		REMARKS
		V (volts)	P (psi)	V (volts)	P (psi)	
0 Hr.	1	1.21	185	1.21	180	Charge
22.8	1	1.73	590	1.70	585	
0 MIN	16.6	1.21	590	1.24	585	Discharge
10	16.6	1.07	550	1.16	540	
20	16.6	1.05	500	1.06	490	
30	16.6	1.05	445	1.06	440	
40	16.6	1.06	385	1.06	375	
50	16.6	1.05	325	1.06	320	
60	16.6	1.05	270	1.06	260	
70	16.6	1.03	215	1.06	205	
72	16.6	1.02	205	1.05	195	

6. CONCLUSIONS

The NASA Lewis - Astropower asbestos coated inorganic separator material is accepted for use in silver-hydrogen cells. To prevent edge shorting and silver bridging, a .16 cm extension of the separator beyond the electrodes appears to be adequate initially.

The most significant cell design variable is the silver electrode thickness which effects the operating current density for a given discharge duration. For the 1.2 hour discharge period, results indicate that a .076cm (.030") thick silver electrode operating at 35 milliamps per square centimeter is optimum. Experiments with and without electrolyte reservoirs, reveal that the initial performance of silver-hydrogen cell is not effected by this component. This means that one layer of separator material and the silver electrode had sufficient electrolyte inventory to provide normal performance. However, it was demonstrated that the electrolyte reservoir does contribute its share of electrolyte to the cell reaction reducing the overall concentration shift. It would be expected that this would have a positive effect in long term use by virtue of the increase in the electrolyte inventory in the cell and the reduction of concentration shifts that take place. Therefore, the final cells contain reservoirs.

No extended life testing was conducted on the cells, and therefore, questions remain of the long term acceptability of the separator material from a standpoint of silver migration and the effectiveness of the extended separator edge to retard silver bridging. Further, the cells studied contained no provision to minimize electrolyte entrainment losses in the evolving gases. This has been demonstrated to be a problem in nickel-hydrogen secondary cells. Therefore, additional testing should be conducted; and some added provisions should be made to the cell to minimize electrolyte entrainment. The design of 20Ahr lightweight cells resulted in an estimated energy density of 58.7 watt hours per kilogram and .05 watt hours per cubic centimeter.

In the design, it is possible to make further weight reductions by reducing the weight of the electrolyte reservoir and it would be expected that cells could deliver approximately 66 watt hours per pound. Larger capacity cells would show further improvement in energy density, since metal gas secondary batteries are very size dependent and have a high inert to active weight ratio in small capacity sizes. Large cells of the silver-hydrogen system should be capable of energy densities in the 66 to 77 watt hour per pound range. This combined with high rate discharge capabilities, state of charge indication, overcharge capability and reversal capability make it an attractive system. A reasonable near term goal should be operating life in excess of 500 deep

charge, discharge cycles. This would make it a very competitive battery when compared against sealed silver-zinc, nickel-cadmium, and nickel-hydrogen cells.

DISTRIBUTION LIST

NASA

Mr. Ernst M. Cohn, Code RPP
National Aeronautics and Space
Administration
Washington, DC 20546

Mr. R. D. Ginter, Code NE
National Aeronautics and Space
Administration
Washington, DC 20546

Mr. Wm. R. Limberis, Code KC
National Aeronautics and Space
Administration
Washington, DC 20546

Mr. Simon Manson, Code NT
National Aeronautics and Space
Administration
Washington, DC 20546

National Aeronautics and Space
Administration
Scientific and Technical
Information Facility
P. O. Box 33
College Park, MD 20740

National Aeronautics and Space
Administration
Technology Utilization Office
Code KT
Washington, DC 20546

GODDARD

Mr. Floyd Ford, Code 711.2
Goddard Space Flight Center
National Aeronautics and Space
Administration
Greenbelt, MD 20771

Mr. Gerald Halpert, Code 711.2
Goddard Space Flight Center
National Aeronautics and Space
Administration
Greenbelt, MD 20771

Mr. Thomas Hennigan, Code 711.2
Goddard Space Flight Center
National Aeronautics and Space
Administration
Greenbelt, MD 20771

Mr. Charles MacKenzie, Code 711.0
Goddard Space Flight Center
National Aeronautics and Space
Administration
Greenbelt, MD 20771

JOHNSON

Mr. Hoyt McBryar, EP5
Johnson Space Center
National Aeronautics and Space
Administration
Houston, TX 77058

Mr. Barry Trout, EP5
Johnson Space Center
National Aeronautics and Space
Administration
Houston, TX 77058

LEWIS

Dr. J. Stuart Fordyce, MS 309-1
Lewis Research Center
National Aeronautics and Space
Administration
21000 Brookpark Road
Cleveland, OH 44135

Dr. Louis Rosenblum, MS 302-1
Lewis Research Center
National Aeronautics and Space
Administration
21000 Brookpark Road
Cleveland, OH 44135

Mr. Harvey Schwartz, MS 309-1
Lewis Research Center
National Aeronautics and Space
Administration
21000 Brookpark Road
Cleveland, OH 44135

MARSHALL

Mr. Charles B. Graff, EC11
George C. Marshall Space
Flight Center
National Aeronautics and Space
Administration
Huntsville, AL 35812

JPL

Dr. R. Lutwack, MS 198-220
Jet Propulsion Laboratory
4800 Oak Grove Drive
Pasadena, CA 91103

Mr. Lloyd D. Runkle, MS 198-220
Jet Propulsion Laboratory
4800 Oak Grove Drive
Pasadena, CA 91103

Mr. Aiji A. Uchiyama
MS 198-220
Jet Propulsion Laboratory
4800 Oak Grove Drive
Pasadena, CA 91103

AIR FORCE

Air Force Aero Propulsion Lab.
POE-1/W. S. Bishop
WPAFB, OH 45433

Mr. D. Pickett AFAPL/POE -1
Aero Propulsion Laboratory
Wright Patterson AFB, OH 45433

Rome Air Development Center
Attn: TUGG/F. J. Mollura
Griffiss AFB, NY 13441

Mr. Edward Raskind, LCC, Wing F
U. S. AF Cambridge Research Lab.
Hanscom AFB
Bedford, MA 01731

SAMSO/DYAE
P. O. Box 92960
Worldway Postal Center
Los Angeles, CA 90009

AFAPL/POE-1/D. R. Warnock
Wright Patterson AFB, OH 45433

ARMY

U. S. Army Electronics Command
Attn: AMSEL-TL-P
Fort Monmouth, NJ 07703

Commanding Officer
U. S. Army Mobility Equip
Research & Development Center
Electrotechnology Department
Electrochemical Division
Attn: SMEFB-EE
Fort Belvoir, VA 22061

Harry Diamond Laboratories
Attn: A. A. Binderly
Room 300, Building 92
Connecticut Ave. & Van Ness St., NW
Washington, DC 20438

NAVY

Commanding Officer
Naval Ammunition Depot
(305, Mr. D. G. Miley)
Crane, Indiana 47522

Naval Surface Weapons Center
Electrochemistry Division, Code 232
White Oaks, MD 20910

Mr. Albert Himy, 6157D
Naval Ship Engineering Center
Center Bldg., Prince Georges
Center
Hyattsville, MD 20782

Dr. George A. Neece
Code 472
800 N. Quincy St.
Office of Naval Research
Arlington, VA 22217

Mr. Donald O. Newton
Chemical Laboratory
Code 134.7
Mare Island Naval Shipyard
Vallejo, CA 94592

Director, Power Program
Code 473
Office of Naval Research
Arlington, VA 22217

Mr. B. B. Rosenbaum, Code 03422
Naval Ship Systems Command
Washington, DC 20360

Dr. H. Rosenwasser AIR 3100
Naval Air Systems Command
Department of the Navy
Washington, DC 20360

Dr. H. E. Ruskie, NISC-4321
4301 Suitland Road
Suitland, MD 20390

Mr. Albert C. Simon, Code 6171
Naval Research Laboratory
Washington, DC 20375

Mr. J. A. Woerner
Naval Ship R&D Center
Annapolis, MD 21402

PRIVATE ORGANIZATIONS

Mr. Larry Gibson
Aerospace Corp.
P. O. Box 95085
Los Angeles, CA 90045

Dr. E. A. Heintz
Technical Department
Airco Speer Carbon-Graphite
P. O. Box 828
Niagara Falls, NY 14302

Dr. R. T. Foley
Chemistry Department
American University
Massachusetts & Nebraska Aves., NW

Mr. R. A. Knight
Research Division
AMF inc.
689 Hope Street
Stamford, CT 06907

Dr. H. Shalit
ARCO Chemical Co.
Division of Atlantic Richfield Co.
500 South Ridgeway Avenue
Glenolden, PA 19036

Dr. Eugene Y. Weissman
Director
Inorganic-Electrolytic R&D
BASF Wyandotte Corporation
Wyandotte, MI 48192

Dr. Allan H. Reed
Battelle Memorial Institute
505 King Avenue
Columbus, OH 43201

Mr. R. L. Beauchamp
Bell Telephone Laboratories
Murray Hill, NJ 07940

Dr. D. O. Feder, Rm 1E-247
Bell Telephone Laboratories, Inc.
Murray Hill, NJ 07974

Dr. Carl Berger
1625 Laird Blvd.
Town of Mt. Royal
Montreal, Quebec, Canada

Dr. C. Bocciarelli
112 E 2nd Street
Moorestown, NJ 08057

Mr. Sidney Gross
MS 8E-37
The Boeing Company
P. O. Box 3999
Seattle, WA 98124

Professor T. P. Dirkse
Calvin College
3175 Burton Street, SE
Grand Rapids, MI 49506

Professor Ernest Yeager
Department of Chemistry
Case Western Reserve Univ.
Cleveland, OH 44106

Mr. C. E. Thomas
Chrysler Corporation
Space Division
Dept. 2130
P. O. Box 29200
New Orleans, LA 70189

Mr. James Dunlop
COMSAT Laboratories
Clarksburg, MD 20734

Dr. K. B. Keating
Experimental Station, Bldg. 304
Engineering Technology Lab.
E. I. DuPont DeNemours & Co.
Wilmington, DL 19898

Mr. E. P. Broglio
Eagle-Picher Industries, Inc.
P. O. Box 47, Couples Dept.
Joplin, MO 64801

Dr. J. G. Cohn
Engelhard Industries
Menlo Park
Edison, NJ 08817

Dr. Eugene Willihnganz
C & D Batteries
Division of ELTRA Corp.
3-43 Walton Road
Plymouth Meeting, PA 19462

Dr. Fritz R. Kalhammer
Electric Power Research Institute
Box 10412
Palo Alto, CA 94304

Mr. L. Berkowitz
Government Research Lab.
Exxon Research & Engineering Co.
P. O. Box 8
Linden, NJ 07036

Dr. Arthur Fleischer
466 South Center Street
Orange, NJ 07050

The Garrett Corporation
ATTN: P. G. Stone
Suite 515, Cafritz Building
1625 Eye Street, NW
Washington, DC 20006

Mr. P. R. Voyentzie
Battery Business Section
General Electric Co.
P. O. Box 114
Gainesville, FL 32601

Mr. F. T. O'Brien
Direct Energy Conversion Programs
General Electric Company
930 Western Avenue
Lynn, MA 01910

Mr. L. J. Nuttall
Direct Energy Conversion Programs
General Electric Company
930 Western Avenue, 274A4
Lynn, MA 01910

Mr. H. Thierfelder
General Electric
Missile and Space Division
Box 8555
Philadelphia, PA 19101

Dr. J. B. Bush, Jr.
Research and Development Center
General Electric Company
Bldg. K-1 Room 4A28
P. O. Box 8
Schenectady, NY 12301

Dr. F. Will
General Electric Company
Research and Development Labs.
P. O. Box 8
Schenectady, NY 12301

Mr. Kenneth Hanson
General Electric Company
Valley Forge Space Technology
Center
P. O. Box 8555
Philadelphia, PA 19101

Mr. J. A. Keralla
Delco Remy Division
General Motors Corp.
2401 Columbus Avenue
Anderson, IN 46011

Dr. G. Goodman
Globe-Union, Inc.
P. O. Box 591
Milwaukee, WI 53201

Dr. C. J. Menard
Gould, Inc.
2630 University Avenue, SE
Minneapolis, MN 55414

Dr. B. B. Owens
Gould Inc., Gould Lab.
P. O. Box 3140
St. Paul, MN 55165

Mr. M. E. Wilke, Chief Eng.
Burgess Battery Division
Gould, Inc.
Freeport, IL 61032

Grunman Aerospace Corp.
S. J. Gaston, Plant 35,
Dept. 553
Bethpage, LI, NY 11714

The Librarian
Livingston Electronic Lab.
Honeywell Incorporated
Montgomeryville, PA 18936

Mr. Robert A. Steinhauer
Hughes Aircraft Co.
Commercial Systems Div.
Bldg. 373 N/S9515
P. O. Box 92919
Los Angeles, CA 90009

Dr. M. E. Ellion, Manager
Propulsion & Power Systems Lab.
Building 366, MS 524
Hughes Aircraft Co.
El Segundo, CA 90245

Mr. R. Hamilton
Institute for Defense Analyses
400 Army-Navy Drive
Arlington, VA 22202

Mr. James R. Hunt
International Nickel Company
1000-16th Street, NW
Washington, DC 20036

Dr. John McCallum
President
Invention Talents, Incorporated
1149 Cheseapeake Avenue
Columbus, OH 43212

Dr. A. Moos
Leesona Corporation
Warwick, RI 02887

Dr. R. A. Wynveen, President
Life Systems, Inc.
24755 High point Road
Cleveland, OH 44122

Dr. James D. Birkett
Arthur D. Little, Inc.
Acorn Park
Cambridge, MA 02140

Mr. Robert E. Corbett
Department 62-25
Building 151/1
Lockheed Aircraft Corporation
P. O. Box 504
Sunnyvale, CA 94088

Mr. S. J. Angelovich
Director of Engineering
Mallory Battery Company
South Broadway
Tarrytown, NY 10591

P. R. Mallory & Company, Inc.
Library
P. O. Box 706
Indianapolis, IN 46206

Dr. Per Bro
P. R. Mallory & Company, Inc.
Northwest Industrial Park
Third Avenue
Burlington, MA 01803

William B. Collins, MS 1620
and M. S. Imamura, MS F8845
Martin-Marietta Corp.
P. O. Box 179
Denver, CO 80201

Mr. A. D. Tonelli
Dept. A3-253, MS 13-3
McDonnell Douglas Astronautics
5301 Bolsa Avenue
Huntington Beach, CA 92647

Dr. Robert C. Shair
Motorola, Inc.
8000 W. Sunrise Blvd.
Ft. Lauderdale, FL 33313

Power Information Center
University City Science
3401 Market Street, Rm 2210
Philadelphia, PA 19104

Me. D. C. Briggs
WDL Division
Philco-Ford Corp.
3939 Fabian Way
Palo Alto, CA 94304

Mr. V. D'Agostino
RAI Research Corporation
225 Marcus Blvd.
Rauppauge, LI., NY 11787

Mr. R. F. Fogle, GA 42
Rockwell International Corp.
Autonetics Division
3370 Miraloma Ave.
Anaheim, CA 92803

Dr. H. L. Recht
Atomics International Division
Rockwell International Corp.
P. O. Box 309
Canoga Park, CA 91304

Rocketdyne Division
Rockwell International Corp.
Attn: Library
6633 Canoga Avenue
Canoga Park, CA 91304

SAFT Corporation
212 Durham Ave.
Middlesex County
Metuchen, NJ 08840

Library
Stanford Research Institute
333 Ravenswood Avenue
Menlo Park, CA 94025

Southwest Research Institute
Attn: Library
P. O. Box Drawer 28510
San Antonio, TX 78284

Mr. Werner Luft
TRW Systems Group MS-M1/1208
One Space Park
Redondo Beach, CA 90278

Dr. W. R. Scott (M1-1208)
TRW Systems, Inc.
One Space Park
Redondo Beach, CA 90278

Dr. Herbert P. Silverman
(R-1/2094)
TRW Systems, Inc.
One Space Park
Redondo Beach, CA 90278

United Aircraft Corporation
Attn: Library
400 Main Street
East Hartford, CT 06108

Union Carbide Corp.
Battery Products Division
Development Laboratory Library
400 Main Street
East Hartford, CT 06108

Union Carbide Corp.
Battery Products Division
Development Laboratory Library
P. O. Box 60656
Cleveland, OH 44101

Dr. Robert Powers
Battery Products Division
Union Carbide Corp.
P. O. Box 6116
Cleveland, OH 44010

Dr. Frederick Morse
Department of Mechanical
Engineering
University of Maryland
College Park, MD 20742

National Center for Energy
Management & Power
260 Towne Building
University of Pennsylvania
Philadelphia, PA 19174

Xerox Corporation
Electro-Optical Systems
300 North Halstead Street
Pasadena, CA 91107

Yardney Electric Division
82 Mechanic Street
Pawcatuck, CT 02891

Yardney Electric Corporation
Power Sources Division
3850 Olive Street
Denver, CO 80207

Giner, Inc.
144 Moody Street
Waltham, MA 02154

EIC
55 Chapel Street
Newton, MA 02158

